

We are IntechOpen, the world's leading publisher of Open Access books Built by scientists, for scientists

6,900

Open access books available

186,000

International authors and editors

200M

Downloads

Our authors are among the

154

Countries delivered to

TOP 1%

most cited scientists

12.2%

Contributors from top 500 universities



WEB OF SCIENCE™

Selection of our books indexed in the Book Citation Index
in Web of Science™ Core Collection (BKCI)

Interested in publishing with us?
Contact book.department@intechopen.com

Numbers displayed above are based on latest data collected.
For more information visit www.intechopen.com



Platinum-Based Alloys and Coatings: Materials for the Future?

Lesley A. Cornish and Lesley H. Chown
*DST/NRF Centre of Excellence in Strong Materials,
and School of Chemical and Metallurgical Engineering,
University of the Witwatersrand,
South Africa*

1. Introduction

Since platinum has a similar chemistry and atomic structure to nickel, platinum-based alloys are possible contenders for partial or complete substitution of nickel-based superalloys. Although the major disadvantages are high price and density, platinum-based alloys have many advantages, including excellent chemical and oxidation resistance and high strength at high temperatures. Since the melting point is higher than nickel, there is potential that Pt-based alloys can exhibit mechanical properties that surpass those of the nickel-based superalloys. Pt-modified coatings are already employed on turbine blades. These can be modified with the addition of different elements and various coating procedures can be used so that the coatings can complement different substrates. This chapter covers the basic properties of a range of Pt-based alloys and describes the different strengthening mechanisms that exist in these alloys, mainly through a structural approach. The oxidation resistance and corrosion resistance are also described. Further, new alloying additions and their effects on the structure and properties are identified.

Nickel-based superalloys (NBSAs) have excellent mechanical properties due to precipitation strengthening. The microstructure comprises many small, strained-coherent, particles of the γ' phase based on Ni_3Al , in a softer matrix of the γ phase, the solid solution (Ni) of nickel (Sims et al., 1987). The strengthening originates from dislocations being slowed down as they negotiate the small ordered γ' particles. There are several mechanisms whereby a unit dislocation has to split into partial dislocations to pass through the ordered precipitates and then re-associate to pass into the random matrix. Each stage requires energy, thus slowing the dislocation movement and providing strengthening. The strengthening depends on the amount of interfacial boundary between the two phases, and is highest when the amount of boundary to be negotiated is highest. This occurs when there are many small precipitates densely distributed, comprising at least 70 vol. % in the alloy (Vattré et al., 2009). For NBSAs, these are usually cubic γ' precipitates aligned on the $\{100\}$ planes (Kear & Wilsdorf, 1962). Additionally, there is solid solution strengthening in the (Ni) matrix, as other elements are dissolved into the nickel, forming a random solid solution. The (Ni) strengthening depends mainly on the difference in elastic and bulk moduli between the Ni and solute atoms (Gypen & Deruyttere, 1981), as well as the size misfit, since each atom varies in size according to its atomic number. There are also bonding effects, all of which make it more difficult for the dislocations to pass.

Although NBSAs are used at high temperatures, significant precipitate coarsening does not readily occur, as the driving force for coarsening is low, due to the low surface energy between the matrix and precipitates (Hüller et al., 2005). Both matrix and precipitates are based on the face centred cubic structure: the γ matrix has a random fcc structure and the γ' particles have an $L1_2$ ordered structure. Aluminium atoms prefer the corners and nickel atoms prefer the faces of the face centred cube. The lattice misfit between these structures is very small and renders the surface energy negligible (Sims et al., 1987), leading to high stability of the fine structure at elevated temperatures, and hence reducing coarsening. Thus, NBSAs are the state-of-the-art material for high temperature, high stress and aggressive environment conditions, with good ductility at both room and high temperatures, and thermal stability.

Although the nickel-based superalloys have excellent mechanical properties, they have nearly reached their temperature limit for operation in turbine engines, unless extreme air-cooling is used, due to the relatively low melting point of nickel (1543°C) and dissolution of the strengthening γ' precipitates at $\sim 1150^\circ\text{C}$. This limits the current operating temperature of NBSAs to $\sim 1100^\circ\text{C}$ (Chen et al. 2009). There have been many developments to increase the temperature capability of these alloys with complex alloying additions and improvements in processing technology and alloy design methodology (Davis, 1997), but in 24 years an increase of only $\sim 100^\circ\text{C}$ has been accomplished, with little scope for any further increases.

The need for increased application temperature arises because turbine engines are more efficient and provide greater thrust at higher temperature. This increased efficiency means less fuel burned, reduced cost as well as reduced CO₂ emissions. Since before 1990, Boeing has halved the mass of emissions by using higher temperature alloys and improved coatings (NIMS, 2007). A number of approaches can be used to obtain higher temperature alloys, including: increased alloying additions to the current nickel-based superalloys, addition of temperature-resistant coatings, or the use of entirely new materials. Since the increase in temperature capability in nickel-based superalloys is constrained by the melting point of nickel, there is interest in developing a whole new suite of similarly structured alloys. These alloys would have higher melting points than the NBSAs for use at temperatures of $\sim 1300^\circ\text{C}$. Potential alloys systems include Mo-B-Si alloys, ceramics, or platinum group metal (PGM) based alloys which have already shown high temperature capability in the glass industry (Selman & Darling, 1973; Roehrig, 1981; Heywood, 1988). However, obstacles to using the PGM-based alloys are their high price and that the conventional alloys show comparably low mechanical resistance at elevated temperatures, although they have been designed with corrosion resistance to the harsh glass-producing environment as their primary attribute.

Platinum-based alloys have high melting points, good thermal stability and thermal shock resistance, and good corrosion- and oxidation-resistance. In several applications, the high electrical and thermal conductivity of Pt are important. Mechanically, Pt alloys combine high ductility with adequate creep strength. These properties give the alloys potential for applications in the chemical industry, space technology and glass industry (Fischer, 2001; Whalen, 1988; Lupton, 1990). In the spacecraft industry, Pt-materials are used to increase the heat resistance of rocket engine nozzles. High-purity optical glasses and glass fibres are manufactured using platinum-containing tank furnaces, stirrers and feeders to withstand high temperatures, mechanical loads and corrosive attack. In glasses, outstanding purity, homogeneity and the absence of bubble inclusions can be achieved only by using platinum. If ceramic melting vessels were used, ceramic particles would be loosened by erosion, contaminating the glass melts and compromising optical properties such as transmittance.

While pure platinum has low mechanical strength at high temperatures, alloying with iridium (Ir) or rhodium (Rh) significantly increases stress rupture strength (Fischer et al., 1997; 1999a and 1999b). These solid solution strengthened alloys have good ductility at high temperatures and can be welded. However, due to evaporation of oxides during annealing above 1100°C in air, Pt-Ir alloys show relatively high mass loss. Conversely, Pt-10%Rh and Pt-20%Rh alloys have a very low evaporation rate. However, grain coarsening in these solid solution strengthened alloys deteriorates the mechanical properties, promoting premature failure of components. To compensate, oxide dispersion strengthened (ODS) Pt-based alloys, with small amounts of finely distributed zirconium or yttrium oxides in the Pt matrix, were developed to improve the high temperature properties (Völkl et al., 1999). The reduction of dislocation mobility and grain boundary stabilisation by the stable oxide dispersoids increased the stress-rupture strength to ~1600°C.

Conventional Pt ODS alloys are manufactured by complicated and expensive powder metallurgical processes (Hammer & Kaufmann, 1982) and exhibit brittleness and susceptibility to cracking. Their low ductility also renders Pt ODS alloys unable to withstand stress concentrations caused by thermal expansion during frequent and rapid temperature changes. Difficulties in fabrication, especially decreased strength due to coagulation of oxide particles after welding, have discouraged the use of ODS platinum alloys (Fischer, 2001). Heraeus (2011) produces ODS Pt-alloys (dispersion hardened platinum DPH® alloys), in a process with internal oxidation, removing the disadvantages of conventional ODS Pt-alloys. These Pt DPH® alloys have good ductility, with comparable oxidation and corrosion resistance to solid solution strengthened Pt-alloys (Merker et al., 2003).

By assessing the applications of a range of Pt alloys, PGMs have been selected as potential base materials in the quest to provide a higher temperature alternative to the Ni-based superalloys. Fischer et al. (1997; 1999a; 1999b; 2001) and Völkl et al. (2000) stated that problems encountered in the aerospace industry could be solved by using Pt-based alloys because they perform exceptionally well in various high-temperature applications, including areas such as glass manufacturing and the handling of corrosive substances (Fischer et al., 2001; Coupland et al., 1980; Hill et al., 2001a). The idea of using an fcc PGM analogue has arisen several times (Bard et al., 1994): in NIMS, Japan with good properties for iridium-based and rhodium-based alloys (Yamabe et al., 1996; 1997; 1998a; 1998b and 1999; Yu et al., 2000), Pt-Ir alloys (Yamabe-Miterai et al., 2003) Pt-Al-Nb and Pt-Al-Ir-Nb alloys (Huang et al., 2004), and platinum-based alloys in South Africa (Wolff & Hill, 2000).

The PGMs and the NBSAs have similar structures (mostly fcc) and similar chemistry for the formation of similar phases. Advantages of PGM-based alloys over the NBSAs are the increased melting temperatures (e.g. 2443°C for iridium, 1769°C for platinum compared to 1455°C for nickel) and the excellent corrosion properties. Although platinum-based alloys are unlikely to replace all NBSAs on account of both higher price and higher density (Pt density of 21.5 g.cm⁻³, compared to Ni density of 8.9 g.cm⁻³), they have potential for use in components subjected to the highest temperatures. For Pt-based alloys, an increase in application temperature of at least 200°C could be gained (and more for Ir-based alloys). Although changes in engine design could be necessary, the higher application temperatures could offset the increased density and expense, and the alloys could be recycled.

Most PGMs are fcc structured, with the exception of ruthenium, which has a hcp structure. Iridium has a higher melting point than platinum, but has the disadvantage of brittleness (Panfilov et al., 2008) and is in short supply. Thus, platinum is the preferred alloy base among the PGMs in the most extreme environments in terms of elevated temperatures,

aggressive atmospheres and higher stresses (Wolff & Hill, 2000; Hill et al., 2001a; Cornish et al., 2003). In terms of coatings, investigations have studied the possibilities that either no coatings would be necessary, or at least simpler coatings could be used than those currently used on nickel-based superalloys (Cornish et al., 2009a, 2009b; Douglas et al., 2009).

Currently, there are three major ranges of Pt-based alloys which have been developed. One is based on Pt-Al-Cr-Ni (Hüller et al., 2005; Wenderoth et al., 2005 & 2007; Rudnik et al., 2008; Völkl et al., 2005 & 2009), and two are based on Pt-Al-Cr-Ru (Cornish et al., 2009a; 2009b; Douglas et al., 2009). Of the latter range, one is more malleable but less resistant to extreme chemical environments, whereas the other has greater chemical resistance, but is more difficult to form. Although no alloys have yet been produced commercially, they are the subject of an ongoing project to develop them further. The major problems in finding a suitable application are that the alloys are too dense for current designs of turbine engines, and that they are extremely expensive. Within these restrictions, the alloys could have potential as coatings on other lighter, more affordable substrates.

2. Rationale for developing Pt-based superalloys

A rationale for the development of the Pt-based superalloys was derived, with the required material structure of fine precipitates in a matrix and using nickel-based superalloys (NBSAs) as the role model. Although Pt-based alloys are used in the glass industry, these did not have the required microstructure, as they were developed primarily for corrosion resistance, rather than strength (Selman & Darling, 1973; Roehrig, 1981; Hammer & Kaufmann, 1982; Heywood, 1988). This meant that there were few platinum alloy systems which could be used as a base for Pt-based superalloys.

Initially, several ternary alloys were produced to identify potential systems on which to base the alloys. The alloys were examined for the required two-phase structure with ordered fcc (cubic L_{12}) phases, and were mechanically tested and tested for oxidation resistance. The first alloys were selected by examining binary phase diagrams (Massalski et al., 1990) containing platinum for the presence of suitable two-phase alloys. From pairs of such binary Pt-alloys, a number of ternary Pt-X-Z alloys were made, where X was a component for precipitate strengthening, and Z was for solid solution strengthening and/or chemical resistance. The alloys were to comprise two-phase microstructures: a γ fcc (Pt) matrix and γ' ordered fcc (L_{12}) Pt_3X precipitates (Hill et al., 2001b, 2001c & 2001d; Cornish et al., 2009a). The candidates for X were: Al, Nb, Ta and Ti, and for Z were: Ni, Re and Ru. Each alloy was first analysed for the required two-phase γ/γ' structure, then was tested for hardness and oxidation resistance. At this stage, an alloy, and its candidate system, was rejected as soon as it failed one of the tests. Thus, alloys were abandoned if they were not two-phase, did not have good mechanical properties, or if they exhibited poor oxidation resistance (Hill et al., 2001b). Although NBSAs are based on $\sim Ni_3Al / (Ni) (\gamma'/\gamma)$, there were two reasons why the Pt-Al system was not chosen at the outset as the basis for the precipitation strengthened alloys. Firstly, Pt_3Al has at least two forms, making the system more complicated than Ni-Al (McAlister & Kahan, 1986; Oya et al., 1987). Secondly, a predisposition to Pt-Al was avoided, in case some other potentially beneficial candidate system was ignored.

Those systems which showed promise became the basis for more detailed studies, involving production of more alloys and further phase diagram studies where necessary. Large losses of niobium showed that the Pt-Nb-Z alloy was insufficiently stable, and the lath-like second

phase containing Nb was incoherent with the matrix, so Nb contents would be limited. Rhenium additions had to be limited to ≤ 3 at.% in order to avoid precipitation of the Re-rich needle-like phase. Two-phase microstructures with a γ fcc (Pt) matrix and γ' ordered fcc (L_{12}) $\sim Pt_3X$ precipitates were achieved in Pt-Ti-X and Pt-Al-X systems, where X is a metal (Hill et al., 2001b). Since the Al-containing alloys had considerably better oxidation behaviour than other alloys, further work focused entirely on Pt-Al-Z alloys. Chromium was found to stabilise the L_{12} cubic form of $\sim Pt_3Al$ and Ru was added as a good solid solution strengthener (Hill et al., 2001d). High temperature oxidation behaviour was found to be suitable, as an external alumina film was formed which protected the alloys, since no internal oxidation occurred during long-term exposure (Hill et al., 2000; Süß et al., 2001a). Simultaneously, work was undertaken on the microstructure and properties of platinum-hafnium-rhodium and platinum-rhodium-zirconium alloys (Fairbank et al., 2000; Fairbank, 2003). The binary Pt_8Hf and Pt_8Zr phases precluded a γ - γ' NBSA analogue in the Pt-Hf and Pt-Zr alloys, because these phases were between the fcc γ and (L_{12}) γ' phases. However, the Pt_8Hf and Pt_8Zr phases did not penetrate far into the Pt-Hf-Rh and Pt-Rh-Zr systems, and γ - γ' regions were formed beyond their limits of penetration. Compressive proof stress results indicated better properties for $Pt_{74.5}:Hf_{17}:Rh_{8.5}$ (at.%) than the initial ternary alloys (Hill et al., 2000), but the oxidation resistance was much poorer.

From these beginnings, two series of Pt-based alloys were developed: Pt-Al-Cr-Ru (Douglas et al., 2009; Cornish et al., 2009b) and Pt-Al-Cr-Ni (Hüller et al., 2005; Wenderoth et al., 2005 & 2007; Rudnik et al., 2008; Völkl et al., 2005 & 2009). Both used the advantageous properties of aluminium (with the added benefit of chromium) for forming the $\sim Pt_3Al$ precipitates and protective alumina films. The former used ruthenium as a solid solution strengthener, whereas the latter alloys used nickel, and avoided ruthenium because of concerns over possible room temperature formation of RuO_4 , a volatile, toxic oxide (Eagleson, 1993). The Pt-Al-Cr-Ni alloys were subjected to more rigorous mechanical testing by the researchers in Germany (Hüller et al., 2005; Wenderoth et al., 2005 & 2007; Rudnik et al., 2008; Völkl & Fischer, 2004; Völkl et al., 2005 & 2009). Further work was done by researchers in South Africa on the addition of alloying elements other than ruthenium to reduce the platinum content and thereby both the expense and the mass (Shongwe et al., 2009; 2010).

Testing of a valuable material requires different testing techniques to those conventionally used. Small samples were produced, usually by arc-melting, with masses of 2–50g, depending on the subsequent testing. Initial characterisation was done on small samples and mechanical properties were determined by performing microhardness tests. Young's modulus can be determined from the hardness values and fracture toughness can be gleaned from the deformation mode, e.g. planar or wavy slip, and cracking around the indentation. Initial oxidation tests could also be done on small samples.

3. Phases and microstructure of platinum-based alloys

As previously stated, platinum has a similar crystallographic structure and chemistry to nickel, and so has similar phase diagrams and hence phase relationships. Since the nickel-based superalloys (NBSAs) are based on the Ni-Al system, with the Ni_3Al precipitates being in a Ni-rich solid solution, a two-phase Pt-Al alloy of similar composition is a good starting point for a NBSA analogue. The Ni-Al and Pt-Al phase diagrams are similar for the Ni-rich and Pt-rich portions (Massalski et al., 1990). Both have fcc solid solutions based on nickel or platinum, and both have eutectic reactions forming Ni_3Al or Pt_3Al , with Ni_3Al being formed

peritectically from NiAl, whereas Pt₃Al melts congruently. This indicates that similar processing in the region where the γ solid solution exists, albeit at higher temperatures, could be utilised to obtain the small γ' Pt₃Al precipitates necessary for the good mechanical properties.

However, there are two important differences between the Ni-Al and Pt-Al systems. One difference is that the limit of the platinum-rich solid solution is less temperature dependent than the nickel-rich solid solution in Ni-Al. This is shown by a comparatively vertical solvus in the binary Pt-Al system, which is a serious disadvantage, as a gradually sloping solvus is necessary for the development of a high proportion of precipitates and precipitation strengthening. However, this can be resolved by further alloying additions, considering that some NBSAs contain up to 15 alloying elements. Alloying additions to Pt-Al have already decreased the slope of the solvus and produced more precipitates. In Pt-Al-Cr-Ni alloys, Wenderoth et al. (2005) attained over 30 vol. % precipitates, thereby deducing that the solvus had to be less vertical than in the Pt-Al binary system.

At elevated temperatures, L₁₂-Pt₃Al does not show an anomalous increase of the flow strength with increasing temperature as exhibited by L₁₂-Ni₃Al (Takeuchi & Kuramoto, 1973), although Pt₃Al should be stronger than Ni₃Al at any temperature (Wenderoth et al., 2005). In the Ni-Al system, Ni₃Al has only one structure, whereas the Pt₃Al phase has at least two (McAlister & Kahan, 1986) if not three (Oya et al., 1987) forms. There are two conflicting phase diagrams regarding the transformation temperatures of γ' Pt₃Al. According to McAlister & Kahan (1986), there is a transformation of the high temperature Pt₃Al phase from L₁₂ to a tetragonal low temperature variant (designated D0'c) at ~1280°C. However, Oya et al. (1987) showed an additional transformation at a lower temperature, with their transformations given as $\gamma' \rightarrow \gamma'_1$ at ~340°C and $\gamma'_1 \rightarrow \gamma'_2$ at 127°C.

The high temperature cubic L₁₂ Pt₃Al allotrope is morphologically identical to L₁₂ Ni₃Al. However, as the lower temperature Pt₃Al allotropes are tetragonal, it is necessary to stabilise the high temperature allotrope. Phase transformations between the cubic and tetragonal allotropes cause a change in volume, leading to local stresses and perhaps premature failure. The presence of the lowest temperature form has been confirmed (Oya et al., 1987), but conditions for its formation have not been fully explained, and may depend on impurities (Douglas et al., 2009) since separate research groups, using different source materials have given different, but reproducible results. Another Pt₃Al allotrope has been recognised in a binary Pt-Al alloy using transmission electron microscopy (TEM) where an unusual ordering phenomenon was found in the Pt₃Al precipitates (Douglas et al., 2007). A similar allotrope has also been calculated using *first principles* (Chauke et al., 2010), showing that the phase relationships are quite complex. This problem would be solved if the high temperature form was stabilised by alloying. The high temperature L₁₂ allotrope has been stabilised and transformations to the lower temperature allotrope(s) inhibited, by small additions of Ti, Ta and Cr (Hill et al., 2001a, 2001e & 2002) and Zr, Hf, Mn, Fe and Co (Hüller et al. (2005).

Two-phase microstructures, leading to considerable precipitation-strengthening, were achieved in Pt-Ti-Z and Pt-Al-Z systems, where Z = Ni, Ru or Re (Hill et al., 2001b). Alloys in these systems showed promising mechanical properties at room temperature, with hardness values higher than 400 HV₁ and high resistance to crack initiation and propagation. However, during annealing at 1350°C for 96 hours, the Pt-Ti-Z alloys reacted with air, precluding further work on these alloys. Further studies were made on the phases and room temperature mechanical properties of Pt-Al-Z alloys after annealing the alloys at 1350°C for 96 hours, where Z = Ru, Re, W, Mo, Ni, Ti, Ta or Cr. Microstructures similar to

Ni- and cobalt- based superalloys were achieved in the Pt-based alloy $Pt_{86}:Al_{10}:Z_4$ (at.%), consisting of cuboidal $\sim Pt_3Al$ precipitates in a (Pt) matrix. Chromium was found to stabilise the cubic form of the $\sim Pt_3Al$ phase, while ruthenium acted as a solid solution strengthener (Biggs et al., 2001; Hill et al., 2001e & 2002). The lowest misfit between the (Pt) and $\sim Pt_3Al$ phases was found at 3-5 at.% Ru and over 20 at.% Al (Biggs, 2001). A lower temperature Pt_3Al form was found in both W- and Ni- containing alloys. In Mo-containing alloys, coarse microstructures were formed and Mo substituted for Pt in the Pt_3Al phase. All the Cr-, Ta- and Ti-containing alloys had favourable microstructures, and the cubic $L1_2$ form of $\sim Pt_3Al$ was stabilised.

Since no ternary Pt-based alloy had the required microstructure with a sufficiently high proportion of γ' precipitates, other alloying additions were needed. Several alloys were made with the objective to increase the γ' volume fraction, and original compositions were selected based on the studies of the ternary Pt-Al-Cr and Pt-Al-Ru systems (Cornish et al., 2009a & b; Douglas et al., 2009). A potential alloy, $Pt_{84}:Al_{11}:Ru_2:Cr_3$ (at%), was composed entirely of a fine two-phase γ/γ' structure, with no primary phase, and its oxidation resistance was superior to the original ternary alloys (Süss et al., 2001b).

Other attempts have been made to improve the properties, and decrease the alloy cost and density by additional alloying elements. Nickel was added to improve the solution strengthening of the (Pt) matrix, although it was not as effective as expected. Cobalt was also added for solid solution strengthening, and extensive phase diagram work was done on the Pt-Al-Co (Chown & Cornish, 2003; Chown et al., 2004) and Pt-Al-Ni systems (Glaner & Cornish, 2003). The Co additions increased the formability. Currently, Nb and V additions are being studied in the hope that they can decrease the Pt content - and hence density and price - while simultaneously increasing the melting point (Shongwe et al., 2009 & 2010).

4. Mechanical properties of ternary pt alloys

4.1 Basis of assessment

As developmental alloys need a comparator, it was decided at the outset that two commercial alloys - MAR-M247 and PM2000 - would be tested. MAR-M247 was selected as a NBSA, and was therefore a representative of the alloys which the platinum alloys might replace. PM2000 was chosen as a comparator because of its advanced microstructure and high-temperature applications. PM2000 is ferrous-based (Fe-Cr-Al) with a ferritic matrix, and is mechanically alloyed with yttrium oxide (Y_2O_3) dispersion material.

4.2 Compressive testing

Ternary substitutional alloying additions to Pt-Al-Z alloys (where Z = Ti, Cr, Ru, Ta & Re) showed that Pt-Al-Z alloys had higher compressive strengths above 1150°C than the commercial NBSA MAR-M247 (Hill et al., 2001c & 2001e). High temperature compressive strength is a useful test for comparison, but it does not equate to creep strength, the latter being a crucial property for most high temperature applications. Using previous results (Biggs et al., 2001; Hill et al., 2001c & 2001e) to select the alloys, creep tests were done at 1300°C on PM2000 and standardised composition $Pt_{86}:Al_{10}:Z_4$ (at.%) alloys, where Z = Ti, Cr, Ru, Ta or Ir, as shown in Figure 1 (Süss et al., 2002). PM2000 had the highest strength of the alloys tested, but the shallow slope of the stress-rupture curve indicated high stress sensitivity and brittle creep behaviour. This indicated that PM2000 would be more likely to fail in the presence of stress concentrations or short overloads during usage. $Pt_{86}:Al_{10}:Cr_4$ exhibited the highest strength of the investigated Pt-based alloys.

Figure 2 shows selected creep curves tested at 30 MPa (Süss et al., 2002). No primary creep stage was seen for the Pt-based alloys within the measurement error. After secondary creep, the Pt-based alloys experienced substantial tertiary creep, leading to fracture strain values between 10 and 50% at 1300°C. It was not possible to resolve different stages of the creep curves for PM2000, because of very low creep rates and fracture strains below 1%. Stress rupture lives of PM2000 and the most promising ternary Pt-based alloy, Pt₈₆:Al₁₀:Cr₄, are shown in Figure 3. Stress-rupture strength values after 10 hours at 1300°C of several conventional solid-solution strengthened Pt-based alloys (Lupton et al., 2000) and zirconia grain stabilised (ZGS) platinum, an oxide dispersion strengthened Pt alloy from Johnson Matthey Noble Metals (Bard et al., 1994) are also shown in Figure 3. The precipitation of γ' particles increased stress-rupture strength, by a factor of 8 from 2.2 MPa for the pure Pt matrix to 17 MPa for Pt₈₆:Al₁₀:Cr₄. The strength of the Pt₈₆:Al₁₀:Cr₄ alloy was also higher than the conventional solution strengthened Pt-based alloys, Pt-10 Rh (wt %) and Pt-20 Rh. By comparing strengths, it can be seen that a rhodium alloying addition of 30 wt% Rh was required for equivalent strength of the Pt₈₆:Al₁₀:Cr₄ alloy. This was encouraging, since the exceptionally high price of Rh and machining difficulties limit the practical use of Pt-30 Rh. At 1300°C, the creep strengths of the Pt-based alloys were higher than those of the Ni- and Co-based superalloys, whose precipitates dissolve at this high temperature, thus losing strength, and were comparable to a platinum ZGS alloy.

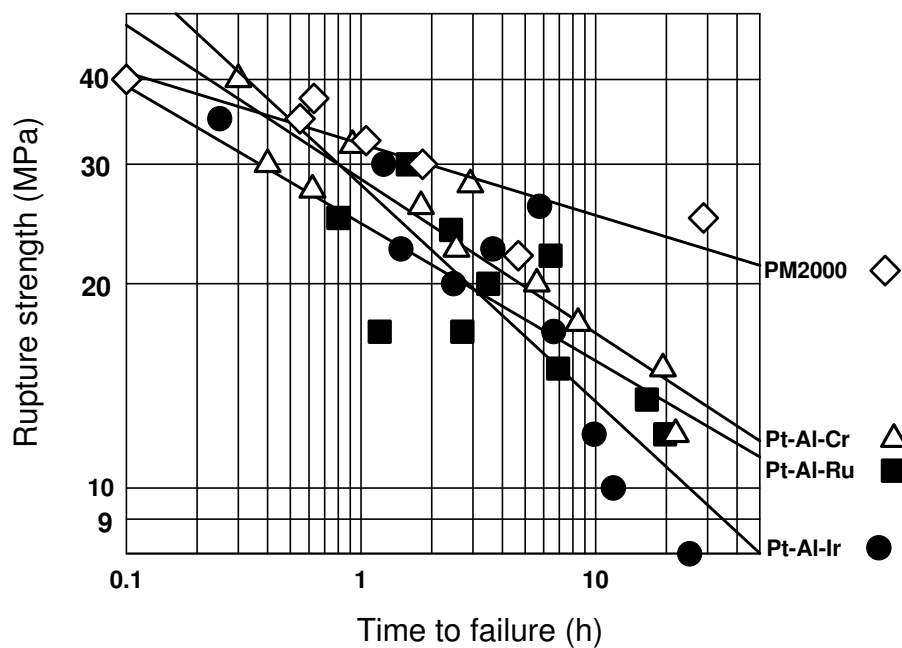


Fig. 1. Stress rupture curves at 1300°C in air of various Pt₈₆:Al₁₀:Z₄ alloys compared to PM2000 (Süss et al., 2002).

In summary, Pt-Al-Z alloys had higher compression strengths above 1150°C than the commercial Ni-based superalloy MAR-M247, and at 1300°C, the Pt-based alloys underwent pronounced tertiary creep leading to fracture strain values of 10-50%. Pt₈₆:Al₁₀:Cr₄ possessed the highest strength of the investigated Pt-based alloys, outperforming several conventional solid-solution strengthened Pt-Rh alloys, and was comparable to Pt ZGS and PM2000. These results were encouraging, as the precipitate volume fraction of ~40% was sub-optimal compared to the ~70% used in commercial NBSAs (Sims et al., 1987).

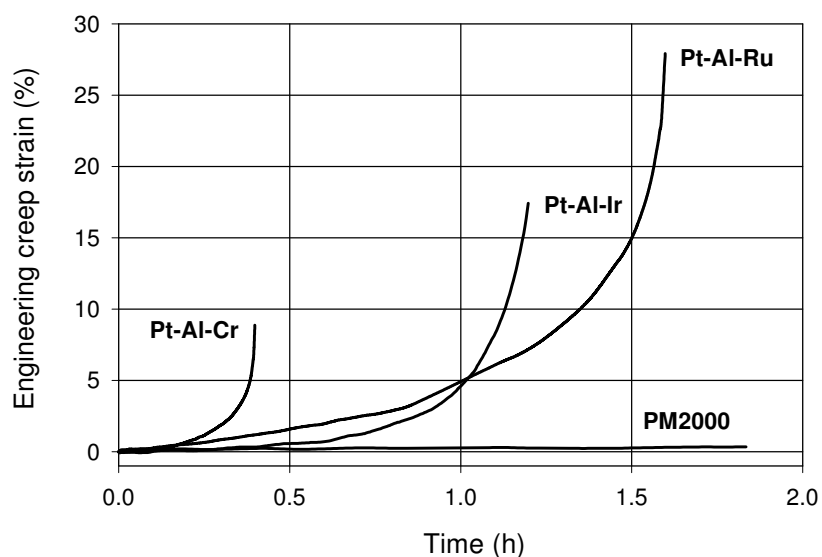


Fig. 2. Creep curves for $Pt_{86}:Al_{10}:Zr_4$ and PM2000 alloys tested at 30 MPa and 1300°C (Süss et al., 2002).

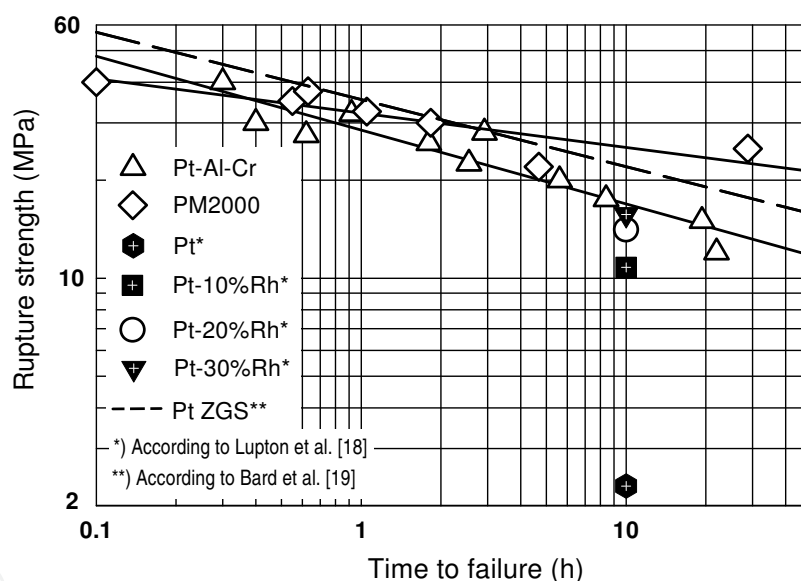


Fig. 3. Stress-rupture lives at 1300°C of $Pt_{86}:Al_{10}:Cr_4$ (at. %), PM2000 and Pt ZGS compared with stress-rupture strength values ($R_{m/10h/1300°C}$) of some conventional solid-solution strengthened Pt-base alloys (Süss et al., 2002.; Lupton et al., 2000; Ochiai, 1994).

Alloys annealed at 1300°C for 96 hours followed by helium quenching gave better all round compression results for $Pt_{80}:Al_{14}:Ru_3:Cr_3$ than $Pt_{86}:Al_{10}:Cr_4$ and $Pt_{86}:Al_{10}:Ru_4$. This was attributed to an increased volume fraction of the $\sim Pt_3Al$ phase, although the precipitates were coarser (Keraan & Lang, 2003a & 2003b; Keraan, 2004).

4.3 Tensile tests

The first tensile tests were undertaken on unoptimised alloys (Süss & Cornish, 2004; Cornish et al., 2009b), although the samples had been heat-treated to promote a homogeneous two-phase microstructure. Since mechanical properties become strain rate dependent at high

temperatures, only the room temperature tensile properties of Pt₈₆:Al₁₀:Cr₄ and Pt₈₆:Al₁₀:Ru₄ ternary alloys were evaluated, and compared with that of the best quaternary alloy, Pt₈₄:Al₁₁:Ru₂:Cr₃. The high temperature compressive strength of Pt₈₄:Al₁₁:Ru₂:Cr₃ was significantly higher than that of Pt₈₆:Al₁₀:Cr₄ (Keraan & Lang, 2003a & 2003b; Keraan, 2004). Macro-scale tensile testing was excluded because of the high material cost. Smaller specimens than the ASTM standard sub-size specimen for tension testing (ASTM E8-93, 1993) were machined, utilising the small specimen test technology and experience from fusion materials development (Lucas et al., 2002). Yield stress is independent of specimen thickness for thicknesses greater than a critical thickness t_c and is not affected by specimen width w , while the ultimate stress is independent of the aspect ratio (t/w) above a critical aspect ratio (t/w)_c (Panayotou, 1982; Kohyama et al., 1987). Specimens were made assuming that a thickness of 3 mm and an aspect ratio of 1 (i.e. a width of 3 mm) would ensure the tensile properties would be independent of the specimen dimensions (Lucas et al., 2002; Kohno et al., 2000). The specimen dimensions were: total length of 46mm and a thickness of 3mm, with a gauge width of 3 mm and gauge length of 18 mm.

After ageing in air at 1250°C for 100 hours followed by water quenching to retain the two-phase γ/γ' structure, flat mini-tensile specimens were machined from each 50g ingot by wire spark erosion. The tensile tests were performed with a cross-head speed of 5 mm.min⁻¹. The maximum ultimate tensile strength and elongation were determined and Vickers hardness tests (HV₁₀) were also performed, with the results given in Table 1. Also shown are the mechanical properties of pure platinum and some commercial high temperature alloys.

Minor cross-contamination of ~0.01 wt% Ru or Cr occurred in some ternary alloys which was probably from sputtering during arc melting. TEM and X-ray diffraction (XRD) showed that, except for the Ru alloys which were 95 vol.% (Pt), all samples comprised (Pt) and ~Pt₃Al (Figure 4). The volume fraction of precipitates varied between specimens.

Alloy composition (at.%)	Reference	Hardness (HV ₁₀)	UTS (MPa)	Elongation (%)
Pt ₈₆ :Al ₁₀ :Cr ₄		317 ± 13	836	~4
Pt ₈₆ :Al ₁₀ :Ru ₄		278 ± 14	814	~9
Pt ₈₄ :Al ₁₁ :Ru ₂ :Cr ₃		361 ± 10	722	~1
Pure Pt - annealed	Johnson Matthey, 2011	40-50	124-245	35-40
Ferritic ODS alloy PM2000	Matweb, 2011	290	720	~14
γ -TiAl	Pather et al., 2003	~250	950	~1
CMSX-4	Maclachlan & Knowles, 2001	~370	870	~4

Table 1. Room temperature mechanical properties of selected Pt-based alloys compared to pure platinum and some commercial high temperature alloys.

Pt₈₆:Al₁₀:Cr₄ had a higher UTS and hardness than Pt₈₆:Al₁₀:Ru₄. Although Pt₈₄:Al₁₁:Ru₂:Cr₃ contained a significant amount of ~Pt₃Al and was the hardest, it had the lowest UTS (Süss & Cornish, 2004). The quaternary alloy failed intergranularly, while the ternary alloys failed mainly by intragranular cleavage, with some localised dimpling. The lower UTS and lower elongation were related to the intergranular failure. This more brittle failure could also have been due to the larger precipitates (Figure 4b), and the unfavourable ogdoadically-diced precipitate morphology (Westbrook, 1958) which is associated with inferior properties (Sims

et al., 1987), especially when compared to $\text{Pt}_{86}\text{Al}_{10}\text{Cr}_4$. These results showed that the microstructure of $\text{Pt}_{84}\text{Al}_{11}\text{Ru}_2\text{Cr}_3$ needed to be optimised (Keraan & Lang, 2003a & 2003b; Keraan, 2004). Since Ru is a better solid solution strengthener than Cr in these alloys (Hill et al., 2001), the higher strength of $\text{Pt}_{86}\text{Al}_{10}\text{Cr}_4$ over $\text{Pt}_{86}\text{Al}_{10}\text{Ru}_4$ was due to the low volume fraction (~5%) of $\sim\text{Pt}_3\text{Al}$ precipitates in $\text{Pt}_{86}\text{Al}_{10}\text{Ru}_4$, showing that it had been annealed above its solvus in the range 1250-1300°C (Süss et al., 2001b). The superior ductility was thus due to its nearly single phase (Pt) nature.

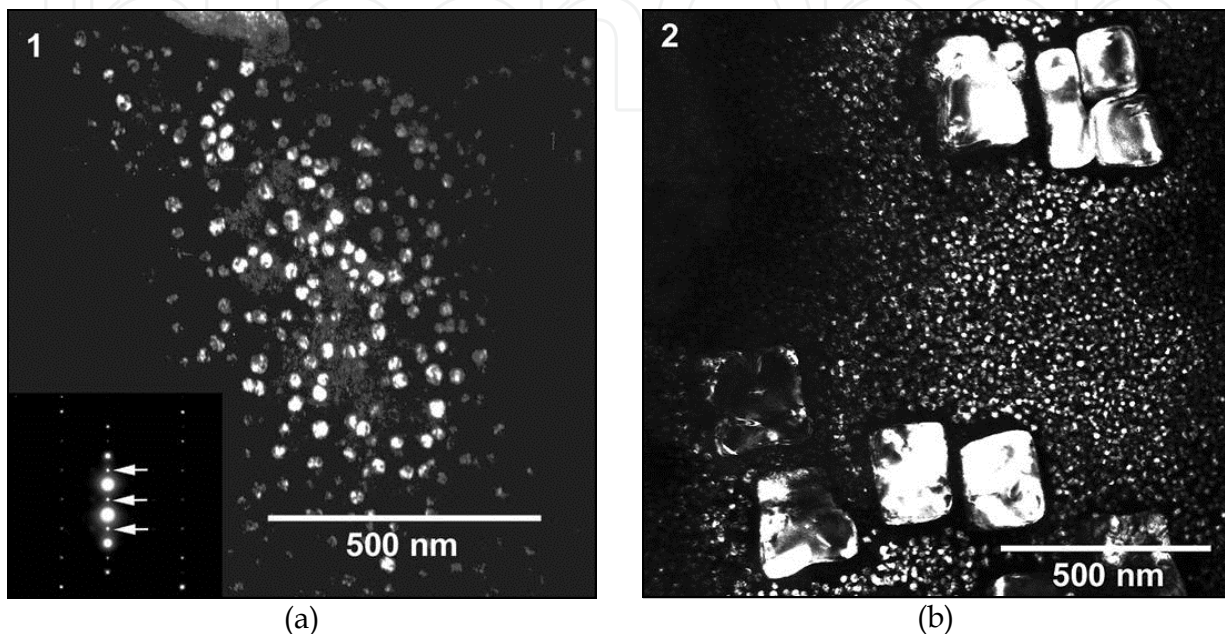


Fig. 4. (a) Dark field TEM image of $\text{Pt}_{86}\text{Al}_{10}\text{Cr}_4$ (Insert: SAD pattern); (b) Dark field TEM image of $\text{Pt}_{84}\text{Al}_{11}\text{Ru}_2\text{Cr}_3$ (Süss & Cornish, 2004; Cornish et al., 2009b).

Although the spread and inconsistencies in the results were disappointing, testing was only undertaken on a small range of specimens due to material expense. As shown in Table 1, the mechanical properties of the tested Pt-based alloys were significantly higher than those of pure Pt in the soft state (Johnson Matthey, 2011). More importantly, the Pt-based alloys showed mechanical properties in a similar range to other high temperature alloys, e.g. ferritic ODS alloy PM2000 (Plansee, 1998), $\gamma\text{-TiAl}$ (Pather et al., 2003) and CMSX-4 (Maclachlan & Knowles, 2001), even though the microstructures were not yet optimised.

Creep test results of $\text{Pt}_{84}\text{Al}_{11}\text{Cr}_3\text{Ru}_2$ were inferior to those of $\text{Pt}_{86}\text{Al}_{10}\text{Cr}_4$, but it was deduced that this was because the former was done in air, whereas initial tests on the latter were done in argon (Cornish et al., 2009b). However, the results of $\text{Pt}_{84}\text{Al}_{11}\text{Cr}_3\text{Ru}_2$ were slightly inferior to those of a commercial dispersion hardening (DPH) Pt alloy. The high temperature compressive strength of $\text{Pt}_{84}\text{Al}_{11}\text{Cr}_3\text{Ru}_2$ was significantly higher than that of $\text{Pt}_{86}\text{Al}_{10}\text{Cr}_4$ (Keraan & Lang, 2003a & 2003b; Keraan, 2004).

Other additions, such as cobalt or nickel, have also been tested to improve the properties of the alloys and decrease their cost and density. Nickel was added to improve the solution strengthening of the matrix, although the intended solution strengthening was not fully achieved. Surprisingly, the melting temperature was increased by Ni additions. The work was not continued because of the disappointingly low hardness results (Glaner & Cornish, 2003), although other research has been more encouraging (Vorberg et al., 2004 & 2005; Hüller et al., 2005; Völkl, et al., 2005; Wenderoth et al., 2005 & 2006).

Pt-Al-Co and Pt-Al-Co-Cr-Ru alloys subjected to cold rolling yielded very interesting results (Chown and Cornish, 2003; Cornish et al., 2009b). Alloys with hardnesses below 400 HV₁₀ showed good formability at room temperature (>75% total reduction in thickness), whereas the formability was poor (<40%) for hardnesses above 450 HV₁₀. The alloys with good formability were two-phase, comprising (Pt,Co) and ~Pt₃Al, with compositions of 5-20 at.% Co and <20 at.% Al. Excellent formability was obtained for alloys containing (Pt) and CoPt₃, whereas the alloys containing other intermetallic compounds showed extremely poor formability (<5% total reduction). The formability of the Pt-Al-Co alloys improved sigmoidally with increased Pt+Co content in the tested range of 60-90 at.% (Pt+Co). The cold formability of these alloys was far superior to other Pt-Al alloyed with Cr, Ru or Ni.

4.4 Developments at Fachhochschule Jena and the University of Bayreuth, Germany

4.4.1 Quaternary Pt-Al-Cr-Ni alloys

The University Bayreuth and the Fachhochschule Jena-University of Applied Sciences in Germany were already researching NBSAs in the 1990s. However, the basis for their development programme on precipitation hardened Pt alloys was the ternary Pt-Al-X alloys being investigated in South Africa (Süss et al., 2002). The Pt₈₆:Al₁₀:Cr₄ composition, with good properties (Figure 3), was the foundation for further work (Wenderoth et al., 2005; Vorberg et al., 2004 & 2005).

Nickel was added to a Pt-Al-Cr alloy in varying amounts (Hüller et al., 2005) since nickel has a good solid-solution strengthening effect on the (Pt) matrix (Zhao et al., 2002), but also to decrease the Pt content, and thus the density and price of the Pt-based alloys. A very promising microstructure was found in the alloy Pt₇₉:Al₁₁:Cr₃:Ni₇: a homogeneous distribution of L₁₂-ordered ~Pt₃Al precipitates with edge lengths of 200-500 nm and volume fraction of 23%. Ageing for 120 h at 1000°C gave a lattice misfit of about -0.1 %, which is in the same range as in commercial Ni-based superalloys.

Based on these results, Pt-Al-Cr-Ni alloys with an increased Al content (Wenderoth et al., 2005), near the solubility limit of ~15 at.% Al (Oya et al., 1989) were made to increase the γ' volume fraction. A two-step heat treatment under flowing argon was used: homogenisation at 1500°C for 12 h, followed by water quenching; then a precipitation heat treatment (ageing) at 1000°C for 120 h, also followed by water quenching. Despite heat treatments being undertaken in flowing argon, there was 6 ppm by volume of residual oxygen, which was sufficient to form an oxide layer 10 μ m thick on the sample surfaces.

Very fine γ' precipitates formed throughout the alloys from the supersaturated matrix during quenching after ageing, although much coarser γ' precipitates were found at a depth of 100 μ m beneath the surface oxide layer (Wenderoth et al., 2005). The concentration profile showed a decrease of Al and an increase of Ni and Pt from the sample interior to the surface. Alloying the Pt-Al system with both Cr and Ni consistently stabilised the L₁₂ high temperature allotrope of Pt₃Al at room temperature. The Pt₈₆₋₇₆:Al₁₁:Cr₃:Ni₀₋₁₀ alloys were all single phase after solution heat treatment at 1450°C, and ageing at 1000°C produced microstructures analogous to Ni-based superalloys. In alloys with less than 6 at.% nickel, precipitates lost coherency after ageing, resulting in spherical particles. Pt₈₀:Al₁₁:Cr₃:Ni₆ had the highest γ' volume fraction (~23%) after ageing, and well-aligned cuboidal precipitates with 0.2-0.5 μ m edge lengths and a misfit of -0.1%. The γ' shapes were due to a decreasing absolute misfit with increasing Ni content. Ageing at 1100°C produced coarse γ' particles and reduced the γ' volume fraction. The volume fraction was less affected by temperature in Ni-containing alloys than in Ni-free alloys.

4.4.2 Variation of the Al content for high γ' volume fraction

Pt-Al_x:Cr₃:Ni₄₋₈ alloys were produced with 12–15 at.% Al (solubility limit is ~15 at.% Al) to increase the γ' precipitate volume fraction (Wenderoth et al., 2005). Alloys with up to 13 at.% Al were successfully homogenised in the single phase γ -region at 1500°C, but at higher Al contents the interdendritic eutectic formed, even after heat treatment at 1530°C.

Homogeneous distributions of \sim Pt₃Al particles were achieved by ageing alloys with up to 13 at.% Al for 120 h at 1000°C. The absolute lattice misfit between γ and γ' decreased with increasing nickel content. Coherency between the γ and γ' phases was shown in alloys with >5 at.% Ni by slightly negative misfit values at room temperature, together with cubic or spherical particles (Figures 5b and c). Conversely, there was limited coherency and a high negative misfit of about -0.5% at nickel contents below 5 at.% Ni (Figure 5a).

Nickel has a smaller atomic radius than platinum (Schubert, 1964). When Ni additions partition to the γ matrix, the γ lattice parameter decreases more than the γ' lattice parameter, lowering the absolute lattice misfits. By increasing Ni, the γ' morphology changed from irregular shaped particles to almost perfect cubes, then to spherical particles, due to the decreasing absolute misfit. Low lattice misfit leads to spherical γ' particles (Qiu, 1996), and in the Pt₇₇:Al₁₄:Cr₃:Ni₆ alloy, medium lattice misfits led to cubic γ' particles. High lattice misfit, as in Pt₇₉:Al₁₄:Cr₃:Ni₄, caused loss of coherency, explaining the irregularly-shaped γ' particles.

As in the ternary alloys (Süss et al., 2002), there was a bimodal distribution of the precipitate sizes: coarse precipitates of ~400 nm length and smaller precipitates of ~100 nm length (Wenderoth et al., 2005). Mean γ' precipitate sizes were 520 nm in Pt₇₇:Al₁₄:Cr₃:Ni₆ and 660 nm in Pt₇₅:Al₁₄:Cr₃:Ni₈ - larger than in Pt-Al-Cr-Ni alloys with 11 at.% Al, which showed maximum sizes of 500 nm after equivalent ageing. (Hüller et al., 2005).

4.4.3 Variation of the Cr γ' volume fraction

The composition of Pt-Al_{12.5}:Cr₀₋₆:Ni₆ was selected to ensure coherency between γ and γ' (Wenderoth et al., 2005). Dendritic as-cast structures of Pt-Al_{12.5}:Cr₃:Ni₆, Pt-Al₁₂:Ni₆ and Pt-Al₁₂:Cr₆:Ni₆ were homogenised by heat treatment at 1500–1510°C, but γ' formation was almost completely suppressed in Pt-Al_{12.5}:Cr₃:Ni₆ after homogenisation for 12 h at 1500°C followed by water quenching. Air cooling produced homogeneous distributions of γ' Pt₃Al particles with 200nm average edge lengths and a volume fraction of about 30%, as shown in Figure 6b. Furnace cooling from 1500°C gave rise to a bimodal particle distribution, and a total γ' volume fraction of 34%. Increasing the Cr content to 6 at.% led to average edge lengths of 500nm and a volume fraction of 50% in Pt-Al₁₂:Cr₆:Ni₆ after homogenisation for 6 h at 1500°C + 6 h at 1510°C in Ar, followed by air cooling. Thus, with controlled air cooling after solution heat treatment, good microstructures were achieved.

Most precipitation strengthened alloys are generated from an eutectic system, and alloys are usually optimised by homogenisation (solution annealing) just below the eutectic temperature in the single phase field of the matrix. Highest strengths are attained with compositions near the solubility limit of the precipitate-forming elements in the matrix (Wenderoth et al., 2005). As-cast Pt-Al-Cr-Ni alloys with 11 at.% Al contained low volume fractions of γ/γ' eutectics, and were successfully solution treated at 1450°C, although annealing at 1400°C was insufficient to produce a single-phase microstructure. Ageing at 1000°C gave a maximum γ' volume fraction of ~23 % for Pt₈₀:Al₁₁:Cr₃:Ni₆ (Hüller et al., 2005). As-cast alloys with 13 at.% Al had dendritic structures with high volume fractions of the γ/γ'

eutectic. Rapid cooling (in the water-cooled copper hearth of the arc furnace) did not prevent secondary precipitation, indicating rapid γ' nucleation and initial growth.

The dendritic structures were converted to fine, homogeneous γ' particles in the γ matrix by solution heat treatment for 12 h at 1500°C and water quenching. Secondary precipitation of γ' occurred despite rapid cooling, which agreed with previous work on other Pt-based alloys (Wolff & Hill, 2000; Vorberg et al., 2004). Precipitation of fine γ' particles within the γ matrix channels has also been seen in NBSA CMSX-10 after multi-step ageing heat treatment (Erickson, 1995), improving the lower temperature tensile and creep strengths.

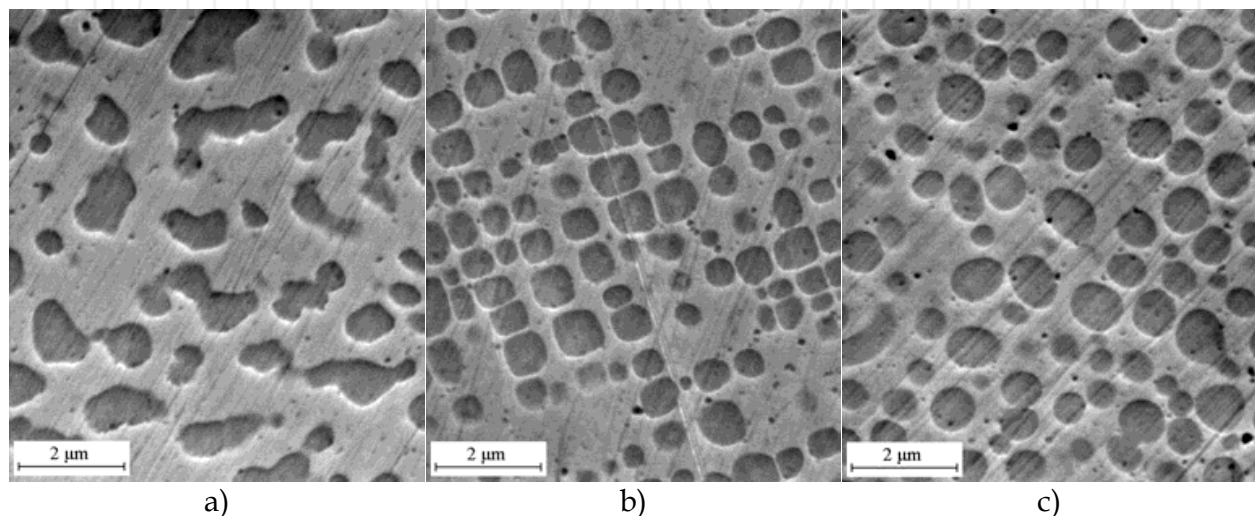


Fig. 5. Secondary electron SEM micrographs of the Pt-based alloys, showing $\sim\text{Pt}_3\text{Al}$ γ' precipitates (dark) in the (Pt) γ matrix (Hüller et al., 2005): a) $\sim\text{Pt}_{79}:\text{Al}_{14}:\text{Cr}_3:\text{Ni}_4$, b) $\sim\text{Pt}_{77}:\text{Al}_{14}:\text{Cr}_3:\text{Ni}_6$, and c) $\sim\text{Pt}_{75}:\text{Al}_{14}:\text{Cr}_3:\text{Ni}_8$ (at. %). [Annealed for 12 h at 1500°C, then 120 h at 1000°C in Ar. Electrolytically etched in 5% aqueous potassium cyanide (KCN) solution].

The simpler structure of the Ni-rich γ matrix (and by inference, the Pt-rich matrix) gives a much lower yield strength than for γ' , but its misfit-induced compression stresses improve creep resistance during the early stages of tensile creep deformation, as long as coherent γ/γ' interfaces remain (Glatzel & Feller-Kniepmeier, 1989; Müller et al., 1993; Völkl et al., 1998). However, high negative misfit values increase the interfacial energy and thus boost the tendency for precipitate coarsening at high temperatures (Sims et al., 1987). Thus, the alloy $\text{Pt}_{77}:\text{Al}_{14}:\text{Cr}_3:\text{Ni}_6$ with an ambient temperature misfit of -0.3% in the solution heat treated condition and -0.1% in the aged condition, shows great potential (Wenderoth et al., 2005).

4.4.4 Substitution of Ni

Although nickel is beneficial in the reduction of misfit, it has a low melting point, and at least some substitution of high melting elements, such as Nb, Ta and Ti is required for improved high temperature properties (Völkl et al., 2009). XRD verified the fcc γ matrix and L_{12} -ordered γ' Pt_3Al phases in $\text{Pt-Al}_7:\text{Cr}_6:\text{Nb}_5$, $\text{Pt-Al}_7:\text{Cr}_6:\text{Ta}_5$ and $\text{Pt-Al}_7:\text{Cr}_6:\text{Ti}_5$ (at. %). The lattice misfit ratios were in the order of -3×10^{-3} in all alloys, and homogenisation promoted bimodal γ' size distributions. Besides coarse and irregularly shaped particles with a volume fraction of 10-20%, there were small cuboids of $\sim 300\text{nm}$ across. Ageing for 264 h at 1200°C with water quenching, resulted in Nb and Ta being almost equally partitioned to both γ and γ' , whereas Ti partitioned to γ' . The γ' volume fractions after ageing were 34% in Pt-

Al₇:Cr₆:Nb₅, 33% in Pt-Al₇:Cr₆:Ta₅ and 35% in Pt-Al₇:Cr₆:Ti₅ (Völkl et al., 2009). Compression strengths of polycrystalline Pt-Al₇:Cr₆:Nb₅, Pt-Al₇:Cr₆:Ta₅ and Pt-Al₇:Cr₆:Ti₅ were higher than that of Pt-Al₁₂:Cr₅ (Süss et al., 2002). At 800°C, Pt-Al₇:Cr₆:Ta₅ was strongest, whereas at higher temperatures Pt-Al₇:Cr₆:Nb₅ was the strongest. Above 1200°C, Pt-Al₇:Cr₆:Nb₅ and Pt-Al₇:Cr₆:Ta₅ outperformed the single-crystal NBSA CMSX-4. The deformed CMSX-4 samples showed rupture on the outside surface, which was also observed in the Nb- and the Ti-containing Pt-based alloys.

Völkl & Fischer (2004) customised equipment to perform stress-rupture tests at high temperatures. At 1300°C, Pt-Al₁₂:Cr₆:Ni₅ had higher stress rupture strengths than both Pt-10%Rh and Pt-10%Rh DPH (Völkl et al., 2009). A Norton plot was generated by plotting minimum creep rate against stress in a double logarithmic plot. This shows data points on near straight lines, where the slope is the Norton exponent n of the Norton creep law:

$$\varepsilon_{\min} = A \sigma^n \quad (1)$$

where: A = a constant which depends on temperature, material and its condition

σ = stress in MPa, n = Norton exponent

The Norton exponent of Pt-10%Rh at 1600°C was calculated as $n = 3.3$ and $A = 34$, the values for pure Pt were $n = 3.8$ and $A = 10.5$ under similar conditions and the Norton exponent of Pt₇₇:Al₁₂:Cr₆:Ni₅ was 3.6 (Völkl et al., 2009). The low Norton exponents for pure Pt, Pt-10%Rh and Pt-Al₁₂:Cr₆:Ni₅ are typical for the viscous-drag controlled creep of single-phase solid solution alloys. However, the low value of Pt-Al₁₂:Cr₆:Ni₅ could also be explained by the intergranular fracture observed in the creep-deformed samples, indicating some brittleness and weakness of the grain boundaries, which has also been found in Pt₈₄:Al₁₁:Ru₂:Cr₃ (Süss & Cornish, 2004; Cornish et al., 2009b). To alleviate this weakness, very small amounts of boron were added, because B tends to segregate to grain boundaries and alters grain boundary adhesion. Rhenium is very beneficial for the creep strength of Ni-based superalloys (Sims et al., 1987), so both B and Re were added to Pt-Al₁₂:Cr₆:Ni₅. Compression creep tests at 1200°C showed that minor B additions increased both creep strength and ductility considerably, and 0.3 at.% B with 2 at.% Re further increased creep strength. Rhenium was found to retard precipitate growth and to increase creep strength (Völkl et al., 2009).

5. Relation of deformation to microstructure

In order to understand the effect of composition on the γ' \sim Pt₃Al precipitates and their deformation, TEM was done on Pt₈₆:Al₁₀:X₄ ternary alloys, where X was Ru, Cr, Ta, Ti and Ir (Hill et al., 2001c; Douglas et al., 2001; Santamarta et al., 2003). The precipitate distribution was bimodal, which could even have been interpreted as trimodal. Ti, Cr and Ta partitioned to \sim Pt₃Al, and stabilised the higher temperature L₁₂ structure of the Pt₃Al phase, resulting in cuboid precipitates (Figure 6a). Conversely, Ru and Ir stabilised a lower temperature modified D0'_c type lath structure. This was recognised as originating from the displacive cubic \sim Pt₃Al \rightarrow tetragonal \sim Pt₃Al reaction (McAlister & Kahan, 1986; Oya et al., 1987), since there were distinct bands (twins) in the precipitates (Douglas et al., 2001, 2003 & 2007; Santamarta et al., 2003; Douglas, 2004). These precipitates often had more complex appearances (Figure 6b), such as ogdoadically-diced shapes identified by Westbrook (1958). The amount of ruthenium in any alloy would need to be balanced to provide both beneficial solid solution strengthening and corrosion resistance properties (Potgieter et al., 1995; van

der Lingen & Sandenbergh, 2001; Shing et al., 2001), without the disadvantage of stabilising the lower temperature \sim Pt₃Al forms, although chromium could be used to offset the latter effect (Hill et al., 2001a, 2001e & 2002).

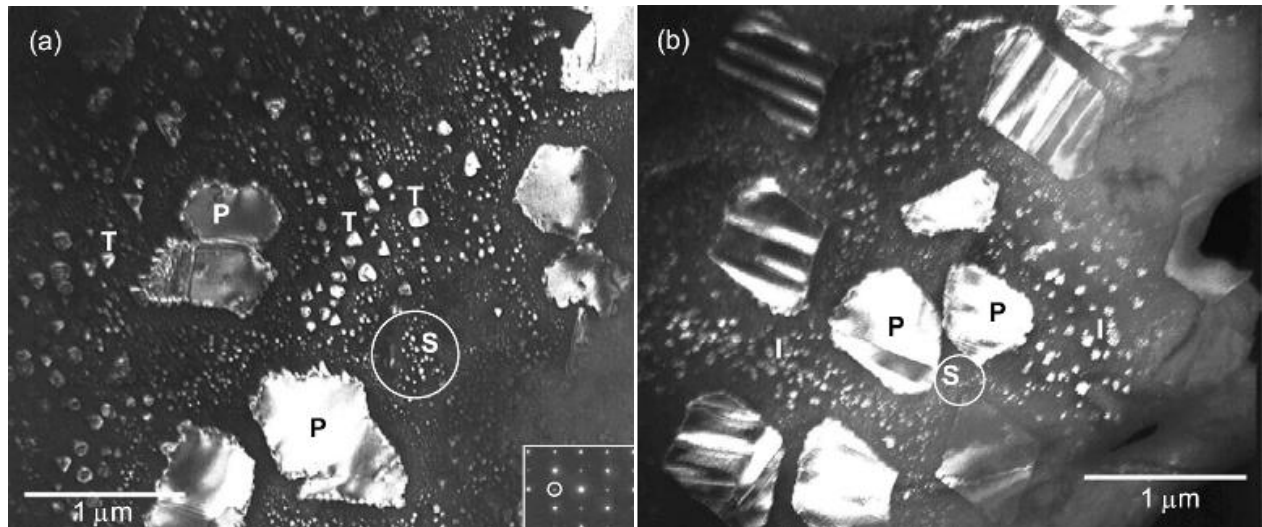


Fig. 6. a). Typical TEM micrograph of the L₁₂ Pt₃Al precipitates stabilized by Cr, Ta and Ti addition. Inset shows the selected area diffraction (SAD) pattern, confirming the L₁₂ structure. b). Typical TEM micrograph of the D0'c precipitates stabilised by Ru and Ir additions. P, T, I and S indicate the different size ranges of the precipitates (Hill et al., 2001c).

Lattice parameters were measured by XRD, using the (220) peak for (Pt) lattice parameters, (112) for tetragonal D0'c Pt₃Al, and (211) for cubic L₁₂ Pt₃Al. The misfit δ was calculated (Sims et al., 1987) using the expression:

$$\delta = 2 \cdot \frac{(a_{\text{ppt}} - a_{\text{matrix}})}{(a_{\text{ppt}} + a_{\text{matrix}})} \quad (2)$$

where a is the lattice parameter.

Table 2 shows misfits at room temperature and 800°C between the matrix and precipitate phases (Hill et al., 2001c). All misfit values were negative, with the smaller misfits arising from the L₁₂ precipitates, and the larger misfits belonging to the transformed D0'c structure. Since the interaction between dislocations in the matrix and precipitates determines the mechanical properties, dislocations were studied and compared to those in nickel-based superalloys (Douglas et al., 2001 & 2003). To simplify the process of understanding the above mechanisms, only ternary alloys were studied. The alloys were Pt₈₆:Al₁₀:X₄ (where X = Cr, Ru, Ti, Ir and Ta) compressed at different temperatures (21, 800, 1000 or 1300°C) (Douglas et al., 2004 & 2009). Lattice parameters of the (Pt) matrix were determined by using selected area electron diffraction (SAED), from <112> zone patterns. Slightly different results from Hill et al. (2001c) were attributed to calibration differences in the microscope cameras. The Burger's vectors were the same as the dislocations in the other alloys.

Pt-Al-Cr: The precipitates were octahedral in shape, not cuboid. With increasing compression temperature, the density of small precipitates decreased, while the dislocation density in the matrix increased. The structure of the dislocation system remained unchanged

and no other slip systems were activated at higher temperatures (Douglas et al., 2004 & 2009).

Alloy	Room temperature			
	$a_{(Pt)}$ (nm)	a_{Pt_3Al} (nm)	δ	Pt ₃ Al type
Pt ₈₆ :Al ₁₀ :Ti ₄	3.8921	3.8642	-0.0072	L1 ₂
Pt ₈₆ :Al ₁₀ :Cr ₄	3.9022	3.8741	-0.0072	L1 ₂
Pt ₈₆ :Al ₁₀ :Ru ₄	3.9001	3.8530	-0.0121	D0'c
Pt ₈₆ :Al ₁₀ :Ta ₄	3.8941	3.8682	-0.0067	L1 ₂
Pt ₈₆ :Al ₁₀ :Ir ₄	3.8983	3.8507	-0.0123	D0'c
	800°C			
	$a_{(Pt)}$ (nm)	a_{Pt_3Al} (nm)	δ	Pt ₃ Al type
Pt ₈₆ :Al ₁₀ :Ti ₄	3.9246	3.8961	-0.0073	L1 ₂
Pt ₈₆ :Al ₁₀ :Cr ₄	3.9390	3.9103	-0.0073	L1 ₂
Pt ₈₆ :Al ₁₀ :Ru ₄	3.9349	3.8967	-0.0098	D0'c
Pt ₈₆ :Al ₁₀ :Ta ₄	3.9246	3.8961	-0.0073	L1 ₂
Pt ₈₆ :Al ₁₀ :Ir ₄	3.9246	3.8747	-0.0128	D0'c

Table 2. Comparative lattice misfits of selected Pt₈₆:Al₁₀:X₄ alloys (Hill et al., 2001c).

Pt-Al-Ru: The precipitates were very different from those observed in Pt-Al-Cr, as they were octahedrally-diced and twinned, originating from the martensitic transformation to tetragonal Pt₃Al. Precipitate interfaces were curved, indicating low surface energies, but at higher compression temperatures the interfaces became increasingly regular. The twin bands also became more developed at higher compression temperatures and dislocations were observed in alternating twin bands. The dislocations occurred in pairs, as expected from the ordering of the precipitates. This is indicative of superlattice dislocations analogous to those in γ' of NBSAs (Douglas et al., 2004 & 2009).

Pt-Al-Ti: After compression at 20°C, the precipitates had well-defined, straight borders, without dislocations, although the matrix contained many dislocation tangles. After compression at 800°C, there were no dislocations within the precipitates, and the dislocation density in the matrix was significantly lower than at ambient temperature. There was also a high density of smaller precipitates in the matrix, adding to the matrix strengthening. Dislocations were only present in the precipitates after compression at 1100°C (Figure 7). The low density of dislocations in the matrix at elevated temperatures indicated significant recovery. At 1300°C, the precipitates were once again dislocation-free, possibly due to recovery (Douglas et al., 2004 & 2009).

Pt-Al-Ir: The precipitates were similar to those in Pt-Al-Ru, as shown in Figure 8. No dislocations were seen in the precipitates, although some dislocations in the matrix extended to the precipitate/matrix interface. After compression at 800°C, the precipitate edges straightened (although their corners were still rounded) and the first dislocations appeared in the precipitates. Isolated dislocations traversed the matrix. At 1100°C, most of the octahedrally-diced precipitates had become spherical. Twin bands were still visible, with dislocation pairs in some, and multiple twinning occurred. At 1300°C, the precipitates were more irregular. The dislocation density was high, with dislocations threading through each twin band and not only through alternating bands, implying that a second slip system had become operative at the higher temperature (Douglas et al., 2004 & 2009).

Pt-Al-Ta: After compression testing at ambient temperature, the precipitates had straight interfaces, with a low density of dislocations within the precipitates and a high density of interfacial precipitates. Isolated tangles of mixed screw and edge dislocations were observed in the matrix. After compression testing at 800°C, irregular precipitates were observed with no dislocations, while the matrix had a high dislocation density with small cubic precipitates. At 1100°C, matrix dislocations disappeared while there were dislocations observed in the more regular precipitates. At 1300°C, the precipitate interfaces were more defined, and the character of the dislocations inside the precipitates was different. From a dislocation viewpoint, this alloy would have the highest strength (Douglas et al., 2004 & 2009), although further testing of the alloy had earlier been abandoned due to poor oxidation resistance (Süss et al., 2001a).

High temperature TEM work: Since the alloys are being developed for high temperature application, the higher temperature cubic allotrope of Pt₃Al is preferred, as it has both higher strength and ductility. This required a study of the effect of temperature on the precipitates, especially the stability of the different Pt₃Al phases, and a study of the dislocations to understand the deformation mechanisms. This work was critical to the planning of other alloying additions to Pt-Al. The simplest alloys were chosen: binary Pt₈₅:Al₁₅ and a ternary Pt-Al-Ir alloy. TEM with bright field imaging was performed at elevated temperatures using *in-situ* heating up to 1100°C (Douglas et al., 2004 & 2009), with a heating rate of 10°C.min⁻¹ (5°C.min⁻¹ was used for observing more detailed changes).

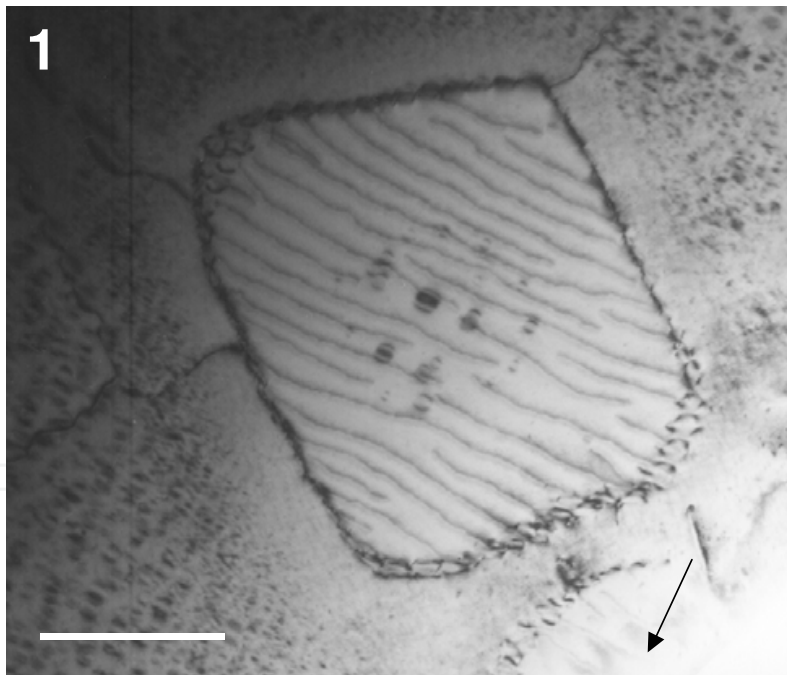


Fig. 7. Bright field TEM micrograph showing the dislocation distribution in a Pt₈₆:Al₁₀:Ti₄ alloy after deformation at 1100°C (scale bar indicates 300nm). (Douglas et al., 2004 & 2009).

At ambient temperature, the precipitates had martensite-like twin bands, with alternating bands having either no dislocations or a high density of dislocations, as would be expected considering the different orientations and dislocation invisibility criteria (Zhang & Zhang, 2001). The dislocation density decreased with increasing temperature and with increasing time. The twin bands disappeared as the crystal structure changed during the phase

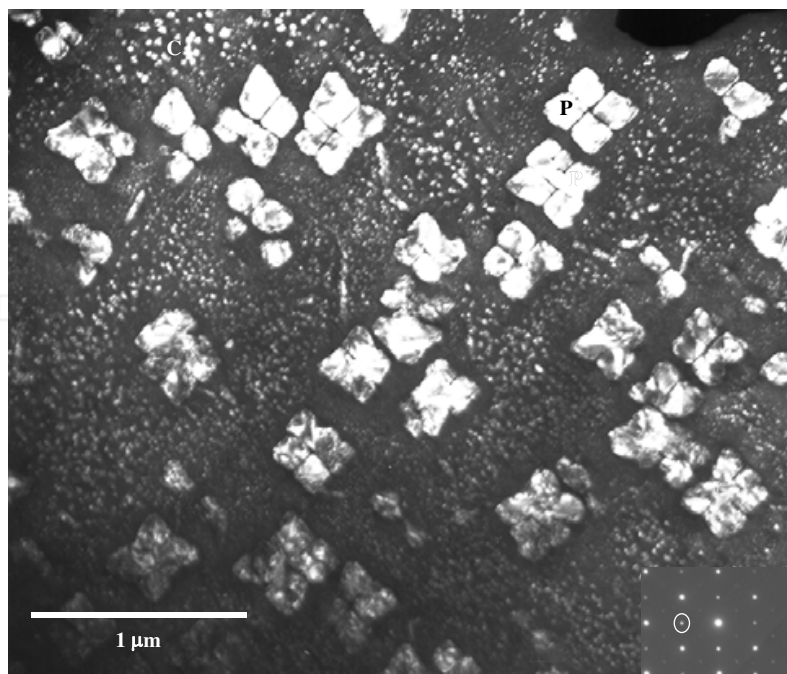


Fig. 8. Dark field TEM micrograph of $\text{Pt}_{86}\text{Al}_{10}\text{Ir}_4$ alloy compressed at room temperature, with P denoting an ovoidally-diced precipitate. The insert shows a SAED pattern with reflection used to obtain image circled. (Douglas et al., 2004 & 2009).

transformation. As a check, the transformation was also observed in diffraction mode (because the diffraction patterns of the two phases are different), and confirmed that the phase diagram of Oya et al. (1987) for the Pt-Al system is more accurate than that of McAlister and Kahan (1986) for these alloys. This was an important result, both because previous attempts to decide which was the most applicable phase diagram - McAlister & Kahan (1986) or Oya et al. (1987) - using SEM, XRD and DTA had been unsuccessful, and because knowledge of the transformation temperatures is vital for application of the alloys.

The strength of a precipitation strengthened alloy depends partially on the small precipitates which reduce dislocation mobility (Kear & Wilsdorf, 1962). To be effective, the precipitates must remain at the high application temperatures to provide a barrier to the dislocation movements. However, in the $\text{Pt}_{85}\text{Al}_{15}$ binary alloy, many of the strengthening precipitates dissolved at high temperatures. There was a high density of small precipitates (and a precipitate-free zone around the large precipitates) in the matrix surrounding the large precipitate at 580°C. At 810°C, the precipitates started to dissolve in the matrix, and between 810°C and 870°C the precipitate dissolution was more rapid, with most of the small precipitates disappearing by 870°C. All small precipitates had dissolved by 960°C, implying reduced precipitate strengthening at high temperatures, although the contributions to strengthening of the various precipitate sizes has not yet been established. The large precipitates were much smaller at 1170°C than at 1030°C, and the interfacial dislocation network had completely disappeared. Thus, other alloying additions are required to increase precipitate stability at high temperatures. This could potentially be achieved with the addition of high melting temperature elements.

The dislocations in the Pt-based alloys were more complex than those in NBSAs, mainly because of the lower temperature form of $\sim\text{Pt}_3\text{Al}$ (γ') and the varying misfits (Hill et al., 2001c; Douglas et al., 2007). However, in the Pt-Al-Cr-Ni system, the dislocations were more similar

to those in NBSAs (Vorberg et al., 2005), indicating that the Pt_3Al precipitates were the fully cubic L_{12} allotrope. In studies on more complex alloys (Rudnik et al., 2008; Shongwe et al., 2008 & 2010), it was found that the relationships between mechanical properties, precipitate size and misfit were difficult to quantify, as different elements acted differently at different compositions, and Ta actually reduced the γ' amount at higher additions, even though it substituted for Al in $\sim\text{Pt}_3\text{Al}$ (Rudnik et al., 2008). The only relationship that was obeyed was that misfit was related to the precipitate morphology, as stated by Qiu (1996).

6. Corrosion studies

6.1 Oxidation of the ternary alloys

Although some alloys with potential for high-temperature applications had already been identified (Hill et al., 2001d), information on high temperature properties was needed. The oxidation resistance was ascertained by a stepped thermogravimetric test, with isothermal holding times of 10 000 s at 900°C, 1100°C, 1300°C and 1400°C. Internal grain boundary oxidation was seen in the Pt-Ti-Ru alloys, and there was extensive internal oxidation in the Pt-Nb-Ru and Pt-Ta-Re alloys. The alloys containing Al exhibited considerably better oxidation behaviour than the other alloys due to the formation of a protective alumina surface layer. Internal oxidation was observed in alloys containing Ti instead of Al, and this was presumed to be the cause of their inferior properties. Thus aluminium is an essential component of the alloys, not only to provide the basis for the precipitation strengthened precipitates, but also to develop the oxidation-resistant alloys (Hill et al., 2001b).

High temperature oxidation behaviour of Pt-Al-Z alloys (where Z = Re, Ta, Ti, Cr, Ir or Ru) was studied by isothermal oxidation tests at 1200°C, 1280°C and 1350°C for at least 100 hours (Hill et al., 2000; Süß et al., 2001a). Results showed increased thickness of the continuous alumina surface layer with time (Figure 10). A dispersion-strengthened alloy, PM2000 (Fe-Cr-Al with a fine dispersion of Y_2O_3 particles in a ferritic matrix) was used as a benchmark. The $\text{Pt}_{86}:\text{Al}_{10}:\text{Ti}_4$ and $\text{Pt}_{86}:\text{Al}_{10}:\text{Ru}_4$ alloys showed similar parabolic oxidation behaviour to the PM2000. The $\text{Pt}_{86}:\text{Al}_{10}:\text{Ir}_4$ and $\text{Pt}_{86}:\text{Al}_{10}:\text{Cr}_4$ alloys showed parabolic behaviour during the early stages of oxidation, with high initial oxidation rates, and subsequent logarithmic growth of the oxide layer, giving these two alloys the thinnest continuous oxide layers after 800 hours exposure.

Following an initial transient period when discontinuous alumina particles precipitated in a Pt matrix, an external alumina film was formed. This occurred because oxygen diffused through the scale more rapidly than the aluminium diffused in the alloy. Only when a critical volume of oxides was reached, did transition from internal oxidation to external scale formation occur (Wood & Stott, 1987). Once formed, the continuous film then provided protection for the alloy, since no further internal oxidation occurred even during long-term exposure. However, the ternary alloys did not perform as well as PM2000, which formed a perfectly continuous oxide layer from the start. Thus, accelerated formation of the continuous alumina layer was found to be necessary. The critical factor was deduced to be a specified minimum amount of aluminium, implying that the protection should increase by increasing the Al content.

The quaternary alloy $\text{Pt}_{84}:\text{Al}_{11}:\text{Ru}_2:\text{Cr}_3$ (at.%) showed improved oxidation resistance to the original ternary alloys (Süss et al., 2001a, 2001b & 2003). The Al content was increased to accelerate oxide scale formation (Süss et al., 2001b). One hour at 1350°C produced a thin continuous oxide layer, and after 10 hours exposure, the scale was already about three times

thicker than the scale layer on $\text{Pt}_{86}\text{Al}_{10}\text{Cr}_4$. No zone of discontinuous surface oxides or any other internal oxidation was observed, as had been seen in some of the earlier Pt-Al-X (where X = Re, Ta and Ti) ternary alloys (Hill et al., 2000; Süß et al., 2001a).

The increased Al content of the alloys accelerated the formation of a continuous alumina layer. Although good properties were achieved for the short test period, the oxidation rates are possibly too high for long application times. Ideally, a continuous oxide layer should form rapidly on the surface, but further mass increase should then follow logarithmic behaviour.

Wenderoth et al. (2007) showed that more complex alloying could promote internal oxidation. A beneficial effect was that Mo, Re and Ru additions reduced the width of the γ' -depleted layer, with Re have the greatest effect.

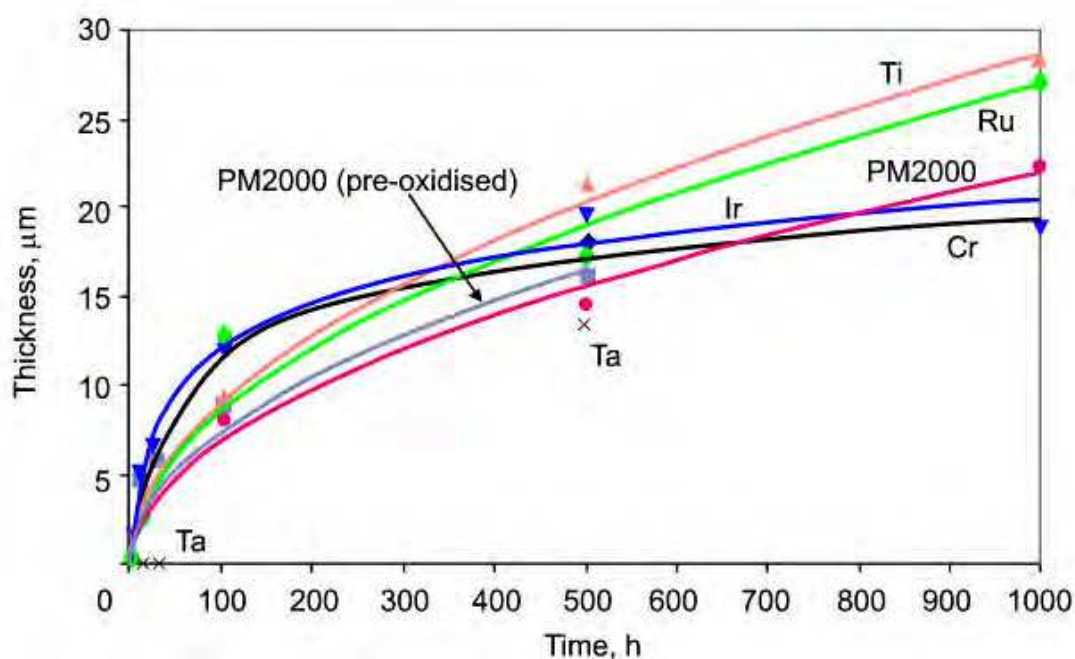


Fig. 10. Isothermal oxidation behaviour of Pt-Al-Z alloys at 1350°C, compared with PM2000 (Süß et al., 2001a).

6.2 Corrosion tests

In addition to high temperature strength, creep resistance and oxidation resistance, high-temperature corrosion resistance is also critical in the selection of high temperature materials (Pint et al., 2006). Increasing application temperatures imply that conditions become increasingly extreme, and materials work closer to their safe operating limits (Elliot, 1989). These conditions cause continued and exacerbated corrosion problems for the high temperature materials. As well as causing catastrophic failures, corrosion has a serious economic impact, as significant time and money is consumed by corrosion-related problems. Improved corrosion control is thus worthwhile, being more economic, safer and extending operational life (Sidhu & Prakash, 2006).

Increasing the high temperature strength of NBSAs was achieved partly by increasing the aluminium and reducing the chromium content, but this increased susceptibility to high temperature corrosion. This was combated by the introduction and development of coatings

(Gurrappa, 2001). Currently, thermal barrier coatings, overlay coatings and diffusion coatings are used in hot section components in the gas turbine as they can withstand temperatures exceeding the substrate melting temperature and protect the substrate from corrosion (Fritscher et al., 1995). However, coatings are expensive and are not completely reliable - catastrophic failure often occurs when coatings are breached. Thus alternatives to coatings are being sought, in particular bulk materials that require no coatings.

Hot corrosion is an aggravated and accelerated form of oxidation that occurs in the presence of sodium sulphate salt (Na_2SO_4) at high temperatures (Eliaz et al., 2002). In turbines, hot corrosion is observed in the low-pressure gas turbine where contaminants can easily accumulate, rather than in the high-pressure turbine. There are two types of hot corrosion: Type I or high-temperature hot corrosion and Type II or low-temperature hot corrosion. Type I hot corrosion usually occurs around 850-950°C, and Type II hot corrosion occurs in the 650°C to 800°C range (Mazur et al., 2005; Sidhu & Prakash, 2006). The main difference between them is their degradation morphology: Type I forms non-porous protective scale with internal sulphidation and chromium depletion, whereas Type II forms a pitted surface with no internal sulphidation. Hot corrosion can increase corrosion loss by up to 100 times (Tsaur et al., 2005), subsequently causing catastrophic failure (Deb et al., 1996). Parameters that affect hot corrosion attack include: material composition, thermomechanical properties, contaminant composition, flux rate, operating temperatures, temperature cycles, gas composition and gas velocity (Potgieter et al., 2010).

A typical test used in the glass industry is the crucible test (Fischer, 1992), where specimens are partially or wholly immersed in fused salt, such as Na_2SO_4 or mixtures of Na_2SO_4 - NaCl , and the attack is rapid and severe. This is an advantageous test for materials in turbines, as Na_2SO_4 is an impurity in air or in fuels, where oxyanions in the molten salt act as the source of sulphur during corrosion attack (Eliaz et al., 2002). The presence of sodium chloride (NaCl) and vanadium pentoxide (V_2O_5) salts aggravates corrosion by forming low-melting eutectic compounds that are extremely corrosive to high-temperature materials (Tsaur et al., 2005; Sidhu & Prakash, 2006). Polarisation techniques are often used in hot corrosion testing of superalloys. Another method of evaluating corrosion is the burner-rig test which more closely simulates the operating environment of turbine engines, and so should be the subject of further work for potential turbine materials (Potgieter et al., 2010).

Four Pt-based alloys and a NBSA CMSX-4 ($\text{Ni-Cr}_{5.7}\text{:Co}_{11}\text{:Mo}_{0.42}\text{:W}_{5.2}\text{:Ta}_{5.6}\text{:Al}_{5.2}\text{:Ti}_{0.74}$) were subjected to a crucible test. Thin discs of the samples were placed in zirconium crucibles, covered in Na_2SO_4 , held in a furnace at 900°C for 168 hours, and weighed periodically (Potgieter et al., 2010). After testing, the corroded surfaces were examined in an SEM, and the corrosion product was analysed using XRD. Results of the alloys are shown in Table 3.

Very little change in mass occurred for the Pt-based alloys. CMSX-4 showed a mass gain followed by a mass loss, and as the sample was almost entirely degraded, the test was discontinued. X-ray diffraction of the corrosion product on CMSX-4 showed a mixture of compounds based mainly on sodium and nickel. Conversely, XRD showed that the surface of the Pt-based alloys mainly consisted of α -alumina -the protective oxide coating that also forms naturally at high temperature.

Alpha-alumina acts as a diffusion barrier, minimising diffusion of substrate elements to the surface (Rhys-Jones, 1989; Müller & Neuschütz, 2003), due to its high thermal stability at high temperatures (Zheng et al., 2006) and low solubility in molten salts (Chen et al., 2003). The presence of α - Al_2O_3 was an indication that the Pt-based substrate was suitably

supporting the alumina layer, as the sample surfaces showed no change in appearance to the naked eye. SEM did show pits in the samples. The alloy Pt₈₆:Al₁₀:Cr₄ was the least affected, and Pt₈₄:Al₁₁:Cr₃:Ru₂ and Pt₈₆:Al₁₀:Ru₄ were slightly pitted, with the latter showing more pits. Pt₇₉:Al₁₅:Co₆ showed a mixture of both more pitted and less pitted areas.

Sample (at.%)	Mass (g)						
	Initial	Day 1	Day 2	Day 3	Day 4	Day 5	Day 6
Pt ₈₆ :Al ₁₀ :Cr ₄	0.611	0.613	0.612	0.611	0.612	0.612	0.612
Pt ₈₆ :Al ₁₀ :Ru ₄	0.478	0.477	0.478	0.479	0.479	0.479	0.478
Pt ₈₄ :Al ₁₁ :Cr ₃ :Ru ₂	0.522	0.524	0.523	0.524	0.522	0.522	0.522
Pt ₇₉ :Al ₁₅ :Co ₆	0.600	0.600	0.600	0.600	0.601	0.601	0.601
CMSX-4	4.430	4.431	4.596	4.583	N/A	N/A	N/A

Table 3. Mass gain of the samples in the crucible test in Na₂SO₄ at 900°C for 168 hours.

A crucible test was then conducted at 950°C to increase the corrosion kinetics (Potgieter et al., 2010), as hot corrosion is more damaging at this temperature (Elliot, 1990; Yoshida, 1993). Five Pt-based alloys and two single-crystal CMSX-4 superalloy samples were tested. A thin platinum aluminide coating (Pt₂Al - Pt₆₇Al₃₃, in at.%) of ~1.25µm thickness was deposited on one of the CMSX-4 samples, while the other was uncoated. Samples were covered by analytical anhydrous Na₂SO₄ salt, the corrosive electrolyte, inside a furnace with a static dry air environment. The test was performed for 540 hours, with an initial 60 cycles (1 hour of heating to 950°C, 20 minutes of cooling to room temperature), followed by long cycles of 72 hours of heating. Samples were washed free of salt residues, and were then weighed after every cycle.

SEM studies of the samples showed that both coated and uncoated CMSX-4 samples experienced much greater attack than the Pt-based alloys, forming a non-protective porous scale (Potgieter et al., 2010). The Pt₇₃:Al₁₅:Co₁₂ and Pt₇₉:Al₁₅:Co₆ samples showed a disintegrated scale layer, indicating that the scale was not protective in this environment. Pt₈₆:Al₁₀:Cr₄, Pt₈₆:Al₁₀:Ru₄ and Pt₈₄:Al₁₁:Cr₃:Ru₂ had similar appearances, with a very thin oxide film on the surface of the alloys which was not visible using optical microscopy. These films were more tenacious and complete, although apparently porous, and provided more protection against hot corrosion than in the Pt-based superalloys with cobalt. Although this scale protected the substrate against high temperature corrosion, the porous nature allowed some internal attack to depths of ~15µm beneath the scale.

Five Pt-based alloys and CMSX-4 underwent potentiodynamic tests with exposure to Na₂SO₄ solutions of 20 or 80 mass % at 60°C. The rationale of the two solutions was that low concentrations favour the attack in turbines, whereas high concentrations are conventionally used to assess hot corrosion. The potentiodynamic curves were obtained at a polarisation scanning rate of 1 mV.s⁻¹ by ramping from -600 to 1 000 mV for the NBSA, and from -300 to 1 000 mV for the Pt-based alloys. The Tafel slopes were established, and i_{corr} was estimated where these tangents intersected E_{corr} . Since corrosion resistance is proportional to i_{corr} , these values were used as a measure of the corrosion resistance. The results are listed in Table 4, and show that the i_{corr} values were much lower for the Pt-based alloys than for the NBSAs, implying that the Pt-based alloys have higher corrosion resistance.

Alloy composition (at.%)	Solution			
	20% Na ₂ SO ₄		80% Na ₂ SO ₄	
	E _{corr} (mV)	I _{corr} (*10 ⁻⁷ A/cm ²)	E _{corr} (mV)	I _{corr} (*10 ⁻⁷ A/cm ²)
Pt ₈₆ :Al ₁₀ :Cr ₄	51	2.4	20	28
Pt ₈₆ :Al ₁₀ :Ru ₄	41	9.8	9	10
Pt ₈₄ :Al ₁₁ :Cr ₃ :Ru ₂	73	2.6	2	25
Pt ₇₉ :Al ₁₅ :Co ₆	214	2.7	131	34
CMSX-4	-387	2.4	329	113

Table 4. Polarisation results for Pt-based alloys and CMSX-4 in Na₂SO₄ solutions.

7. Comparison of the PGM-based alloys with other targeted materials for high temperature applications

The Pt-based alloys show excellent oxidation resistance with simple alloying, especially compared to other materials which are also being developed for high temperature applications (Figure 11), although the experiments were not undertaken under identical conditions (Zhao & Westbrook, 2003). Although the strength values are comparable with other competitors, once normalised against density they are less encouraging (Figure 12). However, before dismissing the Pt-based alloys, several other factors have to be taken into account. Firstly, the excellent corrosion resistance (Figure 11) shows potential that these materials will need simpler coatings, or possibly no coatings. This would reduce manufacturing cost and time. It is also a safety benefit, as it could avoid the potential catastrophic failures due to breaches in coating integrity. Additionally, the Pt-based alloys are formable, which could enable new component designs, thereby utilising the high strength, but with thinner sections (Zhao & Westbrook, 2003). Even though these properties have yet to be accurately determined, the microstructure and mechanical properties already measured indicate that fracture toughness, impact resistance and fatigue resistance is likely to be high for the Pt-based alloys.

The other materials in Figures 11 and 12 (Zhao & Westbrook, 2003) have other limitations which must also be considered. The silicon carbide composites have relatively low strengths, even on the density-normalised plot (Figure 12), although the impact resistance and the high temperature stability are favourable. There are still problems in combating evaporation of SiO₂ from the surface, although there has been good progress with environmental-barrier coatings. However, the manufacture of complex shapes needs to be optimised. The range of Nb silicide composites has good oxidation resistance, fatigue resistance, high-temperature strength and impact resistance. The fracture toughness is reasonable and the material is castable. Good coatings have also been developed for the composites. However, more work needs to be done to achieve both the high oxidation resistance and high strength for the same composition.

Molybdenum-silicon-boron composites have exceptional high temperature creep strength and yield strength, with good oxidation resistance above ~1000°C, although at intermediate temperatures, the oxidation resistance, fatigue resistance, impact resistance and fracture toughness are poor. Additionally, these composites are difficult to manufacture. The oxide-oxide composites (represented by Al₂O₃/GdAlO₃ in Figures 11 and 12) show excellent high temperature strength and oxidation resistance, with reasonable fracture toughness, but the thermal shock resistance is poor. Thus, taking the favourable properties into account and

even considering the high density, overall the Pt-based alloys have potential for application at high temperatures. The price is high, but in view of the high formability, it has been estimated that the price of a Pt-alloy based turbine would be twice that of a current Ni-based superalloy (Glatzel, 2004).

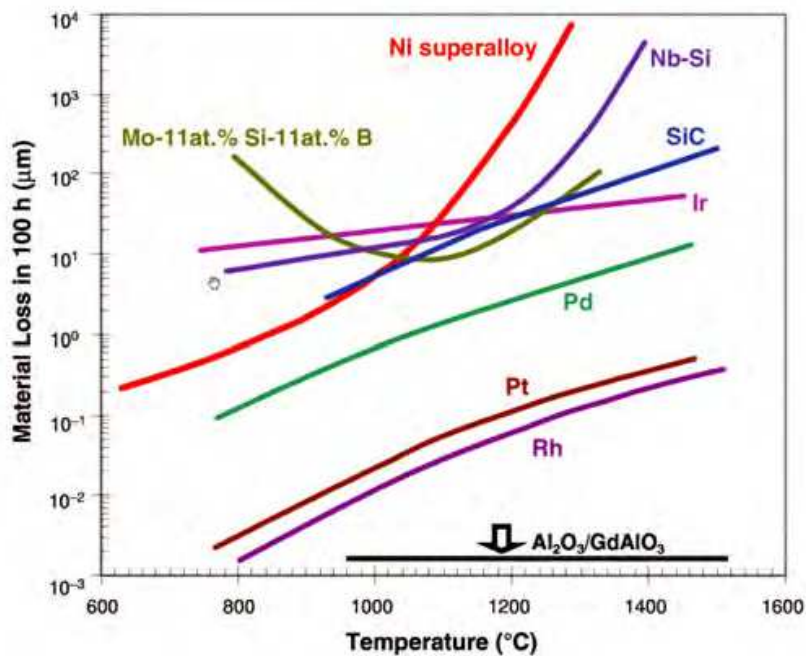


Fig. 11. Oxidation/recession rates of selected high temperature materials (Zhao & Westbrook, 2003). Material loss is usually by formation and spallation of a thermally grown oxide scale, or by evaporation of the metal and oxide. [N. B. The oxidation data were not obtained under identical conditions, so the graph can only be used as a comparison.]

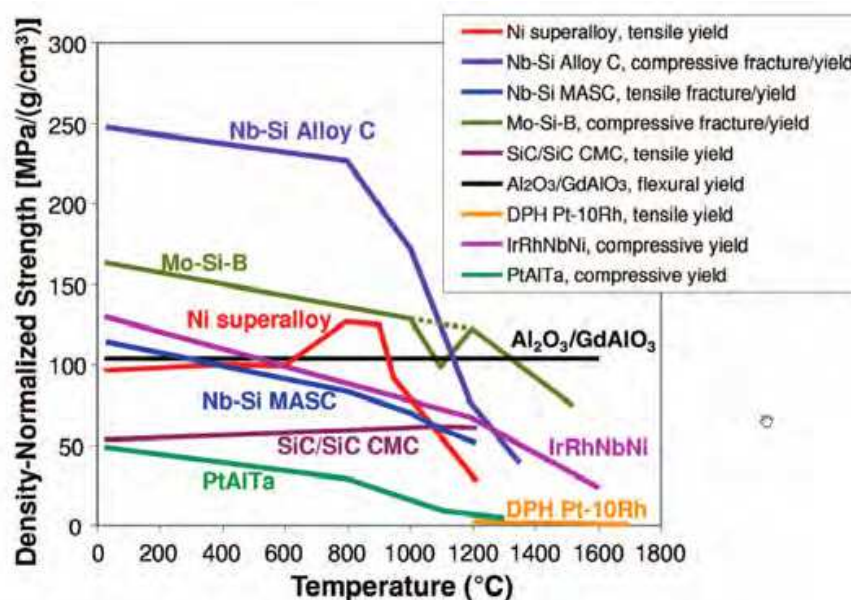


Fig. 12. Comparison of the density-normalised strength graph showing selected potential materials for high temperature applications (Zhao & Westbrook, 2003).

8. Coatings

A second niche is using the Pt-based alloys as coatings on a cheaper substrate, such as a stainless steel. Coatings are employed for a variety of reasons including attractiveness, corrosion resistance and/or wear resistance (although this unlikely for the current alloys). Coatings can be preferable for cheaper components, or where a long component life is not required. Thus, it is more economic to coat a cheaper substrate with a more expensive alloy than to make the whole component from the expensive alloy. Coatings can also be advantageous where low weight is important. The Pt-based alloys are dense, so using them as coatings with the reduced density of a lighter substrate would be beneficial. An added advantage is that the Pt-based alloys form their own enhanced protection in the form of the alumina scale layer.

Pt-modified coatings such as Pt aluminide are preferred for protection against Type I hot corrosion, and have better scale adherence and diffusion protection (Purvis & Warnes, 2001). The addition of other noble metals to Pt-modified coatings is likely to be beneficial, considering the use of such Pt-based alloys for handling molten glass (Fischer et al., 1999b). Coatings are susceptible to thermal cycling and thermal shock. Variations in thermal expansion coefficients promote thermal stresses and possibly subsequent cracking and spallation of coatings. Even the most resistant alloys are susceptible to hot corrosion attacks (Sidhu et al., 2005 and 2006) and no coatings are totally reliable, which can result in catastrophic failure when they do fail. The design of coatings is becoming progressively difficult for increasingly higher temperature applications, due to the lack of compatibility of thermal expansion coefficients between coatings and high-temperature alloys. This further exacerbates the need for new high temperature materials, such as the Pt-based alloys (Wolff & Hill, 2000). However, the high density of platinum might mean that the most likely application would probably be as coatings on suitable substrate materials.

9. Conclusions

Potential NBSA analogues can be made from Pt-based alloys, having an (Pt) fcc solid solution (γ) matrix and $L1_2$ (γ') \sim Pt₃Al precipitates. Although other systems, such as Pt-Ti, were initially tested, the Pt-Al system was identified as the most suitable base in terms of microstructure and mechanical properties. This was attributed to formation of \sim Pt₃Al precipitates which provided strengthening in a softer, formable (Pt) matrix. Additionally, promising oxidation resistance and corrosion resistance were ascribed to the noble metal contents of the alloys and to the protective alumina layer.

Other lighter and cheaper materials are being researched, but all of these have disadvantages and most are very difficult to manufacture. The Pt-based alloys show great promise for high temperature applications despite their high cost and density, as they have good mechanical properties, including formability and oxidation resistance. However, more research needs to be undertaken, as there is much potential for other alloying additions, especially those that could increase the melting temperature and decrease the density, e.g. niobium and vanadium. Further mechanical testing, especially long-term creep testing, should also be undertaken.

10. Acknowledgements

In South Africa, the financial assistance of the South African Department of Science and Technology (DST), the Platinum Development Initiative (PDI) and the DST/NRF Centre of

Excellence in Strong Materials is gratefully acknowledged for the support of the work at Mintek and the University of the Witwatersrand.

11. References

- ASTM Standards (1993). Designation E8-93: Standard Test Methods for Tension Testing of Metallic Metals, *ASTM Standards*, pp. 130-149.
- Bard, J., Selman, G., Day, J., Bourne, A.A., Heywood A.E. and Benedek, R.A. (1994). Dispersion-Strengthened Materials - Platinum-Based Alloys, In: *Mechanical Properties of Metallic Composites*, ed. Shojiro Ochiai, Marcel Dekker Inc., New York, U.S.A., pp. 341-371.
- Biggs, T. (2001). An Investigation into Displacive Phase Transformations in Platinum Alloys, Ph.D. Thesis, University of the Witwatersrand, Johannesburg, South Africa.
- Biggs, T. Hill, P. Cornish L. A. and Witcomb, M. (2001). Investigation of the Pt-Al-Ru diagram to facilitate alloy development, *J. of Phase Equilibria*, Vol. 22, No. 3, pp. 214-215.
- Chauke, H., Minisini, B, Drautz, R, Nguyen-Manh, D Ngoepe, P. and Pettifor D (2010). Theo-retical investigation of the Pt₃Al ground state, *Intermetallics*, Vol. 18, pp. 417-421.
- Chen, Z., Wu, N., Singh, J. and Mao, S. (2003). Effect of Al₂O₃ overlay on hot-corrosion behavior of yttria-stabilized zirconia coating in molten sulfate-vanadate salt, *Thin Solid Films*, Vol. 443, No. 1, p. 46.
- Chen, Z. B., Huang, Z., Wang, Z. and Zhu, S.J. (2009). Failure behavior of coated nickel-based superalloy under thermomechanical fatigue, *J. Mater. Sci. ,* Vol. 44, pp. 6251-6257.
- Chown, L.H. and Cornish, L.A. (2003). The Influence of Cobalt Additions to Pt-Al and Pt-Al-Ru-Cr Alloy Systems, in *Africa Materials Research Society Conference*, University of the Witwatersrand, Johannesburg, 8-11 December 2003, pp. 136-137.
- Chown, L.H., Cornish, L.A. and Joja, B. (2004). Structure and Properties of Pt-Al-Co Alloys, in *Proc. Microsc. Soc. south. Afr.*, Vol. 34, Pretoria, 30 Nov. - 3 Dec. p. 11.
- Cornish, L.A., Fischer B. and Völkl, R. (2003). Development of Platinum Group Metal Based Superalloys for High Temperature Use, *Materials Research Bulletin*, Vol. 28, No. 9, pp. 632-638.
- Cornish, L.A., Süss, R., Douglas, A., Chown, L.H. and Glaner, L. (2009a). The Platinum Development Initiative: Platinum-Based Alloys for High Temperature and Special Applications: Part I, *Platinum Metals Review*, Vol. 53, No. 1, pp. 2-10.
- Cornish, L.A., Süss, R., Chown, L.H. and Glaner, L. (2009b). The Platinum Development Initiative: Platinum-Based Alloys for High Temperature and Special Applications: Part III, *Platinum Metals Review*, Vol. 53. No. 3, pp. 155-163.
- Coupland, D.R., Corti C.W. and Selman, G.L. (1980). The PGM Concept: Enhanced Resistant Superalloys for Industrial and Aerospace Applications, in *Behaviour of High Temperature Alloys in Aggressive Environments*, ed. I. Kirman, Proc. of the Petten International Conf., Petten, The Netherlands, 15-18 Oct. 1979, TMS London.
- Davis, J. R. (1997) *Heat-resistant Materials*, ASM International, pp. 1-591.
- Deb, D., Rama Krishna Iyer, S. and Radhakrishnan, V.M. (1996). Assessment of high temperature performance of a cast nickel base superalloy in corrosive environment, *Scripta Materiala*, Vol. 35, No. 8, pp. 947-952.

- Douglas, A., Neethling, J.H., and Hill, P.J. (2001). Suppression of Martensite Phase in L1₂ Pt-Al Alloys, In *5th Multinational Congress on Electron Microscopy (MCEM5)*, Lecce, Italy, 20-25 Sep. 2001.
- Douglas, A., Neethling, J.H., Santamarta, R., Schryvers D. and Cornish, L.A. (2003). TEM investigation of the microstructure of Pt₃Al precipitates in a Pt-Al alloy, in *Proc. Microsc. Soc. south. Afr.*, Vol. 32, Cape Town, 3-5 December 2003, p. 14.
- Douglas, A. (2004). Microstructure and Deformation of Ternary Platinum Alloys as Superalloy Analogues, Ph.D. Thesis, University of Port Elizabeth.
- Douglas, A., Neethling, J.H. and Cornish, L.A. (2004). Dislocation distribution in a Pt-based analogue of Ni-Based superalloys, in: *Proc. Microsc. Soc. south. Afr.*, Vol. 34, Pretoria, p. 12.
- Douglas, A., Neethling, J.H., Santamarta, R., Schryvers D. and Cornish, L.A. (2007). Unexpected ordering behaviour of Pt₃Al intermetallic precipitates, *J.of Alloys and Compounds*, Vol. 432, pp. 96-102.
- Douglas, A., Hill, P.J., Cornish, L.A. and Süß, R. (2009). The Platinum Development Initiative: Platinum-Based Alloys for High Temperature and Special Applications: Part II, *Platinum Metals Review*, Vol. 53, No. 2, pp. 69-77.
- Eagleson, M. (1993). *Concise Encyclopaedia Chemistry*, Eds. H-D Jakubke and H Jeschkeit, De Gruyter, 1993, p. 960.
- Eliaz, N., Shemesh, G. and Latanision, R.M. (2002). Hot corrosion in gas turbine components, *Engineering Failure Analysis*, Vol. 9, No. 1, pp. 31-43.
- Elliott, P. (1989). "Catch 22" and the UCS Factor - Why Must History Repeat Itself?, *Materials Performance*, Vol. 28, No. 7, pp. 75-78.
- Elliot, P. (1990). Practical Guide to High Temperature Alloys, *Materials Performance*, NACE International, Vol. 28, No. 8, pp. 57-66.
- Erickson, G.L. (1995). A New Third Generation, Single Crystal, Casting Superalloy, *JOM*, Vol. 47, No. 4, pp. 36-39.
- Fairbank, G.B., Humphreys, C.J., Kelly, A. and Jones, C.N. (2000). Ultra-high Temperature Intermetallics for the Third Millennium, *Intermetallics*, Vol. 8, No. 9-11, pp. 1091-1100.
- Fairbank, G. B. (2003). The Development of Platinum Alloys for High Temperature Service, Ph.D. Thesis, University of Cambridge, U.K.
- Fischer, B. (1992). Reduction of Platinum Corrosion in Molten Glass, *Platinum Metals Review*, Vol. 36, No. 1, pp. 14-25.
- Fischer, B., Freund D. and Lupton, D.F. (1997). Stress-Rupture Strength and Creep Behaviour of Platinum Alloys, In *Precious Metals 1997, Proc. IPMI 21st Annual Conference on Precious Metals*, San Francisco, California, USA, 15-18 June 1997, Int. Precious Metals Institute, Pensacola, Florida, USA, pp. 307-322.
- Fischer, B., Behrends, A. Freund, D., Lupton D.F. and Merker, J. (1999a). Dispersion Hardened Platinum Materials for Extreme Conditions, *Proc. of the 128th Annual Meeting and Exhibition of TMS*, San Diego, California, USA, 28 Feb.-4 Mar. 1999, pp. 321-331.
- Fischer, B., Behrends, A., Freund, D., Lupton D.F. and Merker, J. (1999b). High Temperature Mechanical Properties of the Platinum Group Metals, *Platinum Metals Review*, Vol. 43, No. 1, pp. 18-28.

- Fischer, B. (2001). New Platinum Materials for High Temperature Applications, *Advanced Engineering Materials*, Vol. 3, No. 10, pp. 811-820.
- Fritscher, K., Leyens, C. and Peters, M. (1995). Structural materials: properties, microstructure and processing, *Mat. Sci. and Eng. A*, Vol. 190, No. 1-2, pp. 253-258.
- Glaner, L. and Cornish, L.A. (2003). The Effect of Ni Additions to the Pt-Al-Cr-Ru System, in *Proc. Microsc. Soc. south. Afr.*, Vol. 33, Cape Town, 3-5 December 2003, p. 17.
- Glatzel, U. and Feller-Kniepmeier, M. (1989). Calculations of Internal Stresses in the γ/γ' Microstructure of a Nickel-Base Superalloy with High Volume Fraction of γ' -Phase, *Scripta Metallurgica*, Vol. 23, pp. 1839-1844.
- Glatzel, U. (2006). Private communication to R. Süss.
- Gurrappa, I. (2001). Identification of hot corrosion resistant MCrAlY based bond coatings for gas turbine engine applications, *Surf. Coat. Tech.*, Vol. 139, No. 2-3, pp. 272-283.
- Gypen, L. and Deruyttere, A. (1981). The combination of atomic size and elastic modulus misfit interactions in solid solution hardening, *Scripta Metal*, Vol. 15, No. 8, pp. 815-820.
- Hammer, G. and Kaufmann, D. (1982). Degussa AG, *German Patent Appl.* 3,030,751 A1.
- Heraeus (2011). Dispersion Hardened Platinum Materials, Date of access: 22 February 2011. Available from Heraeus website:
http://heraeusptcomponents.com/en/downloads_1/technical_informations/publications_1/
- Heywood, A.E. (1988). Johnson Matthey PLC, *German Patent* 3,102,342 C2.
- Hill, P.J., Cornish, L.A. and Witcomb, M.J. (2000). The Oxidation Behaviour of Pt-Al-X Alloys at Temperatures between 1473 and 1623 K, In: *Proc. High Temperature Corrosion and Protection 2000*, pp. 185-190, 17-22 Sep. 2000, Sappora, Japan, ISBN1-900814-35-8.
- Hill, P. J., Cornish L. A. and Fairbank G. B. (2001a). New Developments in High-Temperature Platinum Alloys, *JOM*, Vol. 53, No. 10, pp. 19-20.
- Hill, P.J., Biggs, T., Ellis, P., Hohls, J., Taylor S. and Wolff, I.M. (2001b). An assessment of ternary precipitation-strengthened Pt alloys for ultra-high temperature applications, *Mat. Sci. and Eng. A*, Vol. 301, No. 2, 167-179.
- Hill, P.J., Yamabe-Mitarai, Y., Murakami, Y., Cornish, L.A., Witcomb, M.J., Wolff, I.M. and Harada, H. (2001c). The Precipitate Morphology and Lattice Mismatch of Ternary (Pt)/Pt₃Al Alloys, In *3rd Int. Symp. on Structural Intermetallics*, TMS, Jackson Hole, Wyoming, U.S.A., Sept, 28 Apr. - 1 May, 2002, pp. 527-533.
- Hill, P.J, Yamabe-Mitarai, Y. and Wolff, I (2001d). High-temperature compression strengths of precipitation-strengthened ternary Pt-Al-X alloys, *Scripta Mat.*, Vol. 44, No. 1, pp.43-48.
- Hill, P.J., Cornish, L.A., Ellis, P. and Witcomb, M.J. (2001e). The Effect of Ti and Cr Additions on Phase Equilibria and Properties of (Pt)/Pt₃Al Alloys, *J. of Alloys and Compounds*, Vol. 22, pp. 166-175.
- Hill, P.J., Adams, N., Biggs, T., Ellis, P., Hohls, J., Taylor, S.S., and Wolff, I.M. (2002). Platinum alloys based on Pt-Pt₃Al for ultra-high temperature use, *Mat. Sci. and Eng. A*, Vol. 329-331, pp. 295-304.
- Huang, C., Yamabe-Mitarai, Y. and Harada, H. (2004). The stabilization of Pt₃Al phase with L1₂ structure in Pt-Al-Ir-Nb and Pt-Al-Nb alloys, *J. of Alloys and Compounds*, Vol. 366, pp. 217-221.

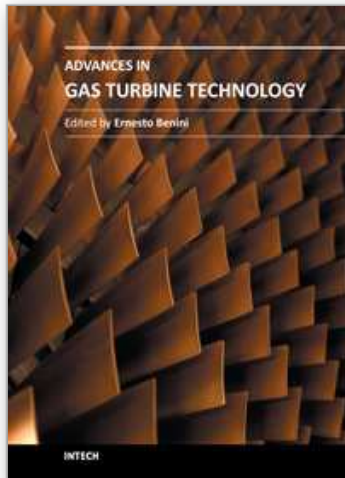
- Hüller, M., Wenderoth, M., Vorberg, S., Fischer, B., Glatzel, U. and Völkl, R. (2005). Optimization of Composition and Heat Treatment of Age-Hardened Pt-Al-Cr-Ni Alloys, *Metall. and Mater. Trans. A*, Vol. 36, No. 13, pp. 681-689.
- Kear B.H. and Wilsdorf, H.G.F. (1962). *Trans TMS-AIME*, Vol. 224, p. 382. Cited in: Vattré, A., Devincere, B. and A. Roos (2009) Dislocation dynamics simulations of precipitation hardening in Ni-based superalloys with high γ' volume fraction, *Intermetallics*, Vol. 17, Issue 12, pp. 988-994.
- Keraan, T. and Lang, C.I. (2003a). High Temperature Investigation into Platinum-base Super-alloys, in *Proc. Microsc. Soc. south. Afr.*, Vol. 32, Cape Town, 3-5 Dec. 2003, p. 14.
- Keraan, T. and Lang, C.I. (2003b). High Temperature Mechanical Properties and Behaviour of Platinum-base Superalloys for Ultra-high Temperature use, In: *Africa Materials Research Society Conference*, University of the Witwatersrand, Johannesburg, 8-11 December 2003, pp. 154-155.
- Keraan, T. (2004). High Temperature Mechanical Properties and behaviour of Platinum-base Alloys, M.Sc. Dissertation, University of Cape Town.
- Kohno, Y., Kohyama, A., Hamilton, M.L., Hiroshi, T., Katoh, Y. and Garner, F.A. (2000). Specimen size effects on the tensile properties of JPCA and JFMS, *J. of Nuclear Materials*, Vol. 283-287, pp. 1014-1017.
- Kohyama, A., Asano, K. and Igata, N. (1987). Influence of radiation on materials properties: *15th Int. Symposium (Part II)*, ASTM-STP 956, p. 111; cited in: Cornish et al., 2009b.
- Johnson-Matthey (2011). Accessed 3 Mar. 2011. Available from: www.platinum.matthey.com
- Kamm, J.L. and Milligan, W.W. (1994). Phase stability in (Ni,Pt)₃Al Alloys, *Scripta Metallurgica et Materialia*, Vol. 33, No. 11, pp. 1462-1464.
- Lucas, G.E., Odette, G.R., Sokolov, M., Spätig, P., Yamamoto, T. and Jung, P. (2002). Recent progress in small specimen test technology, *J. of Nuclear Materials*, Vol. 307-311, pp. 1600-1608.
- Lupton, D.F. (1990). Noble and Refractory Metals for High Temperature Space Applications, *Advanced Materials*, pp. 29-30.
- Lupton, D. F., Merker, J., Fischer, B. and Völkl, R. (2000). Ductile High-Strength Platinum Materials for Glass Making, *Proc. on CD-ROM, 24th Int. Precious Metals Conference 2000*, Williamsburg, USA, 11-14 June, cited by Cornish et al., 2009a.
- MacLachlan D.W. and Knowles, D.M. (2001). Modelling and prediction of the stress rupture behaviour of single crystal superalloys, *Mat.s Sci. and Eng. A*, Vol. 302, pp. 275-285.
- Massalski, T.B., Okamoto, H., Subramanian, P.R. and Kacprzak, L. (Eds.) (1990). *Binary Alloy Phase Diagrams, 2nd Ed.*, ASM International, Ohio, USA.
- Matweb (2011). Date of access: 6 March 2011. Available from: www.matweb.com/
- Mazur, Z., Luna-Ramírez, A., Juárez-Islas, J. A. and Campos-Amezcuca, A. (2005). Failure Analysis of a Gas Turbine Blade Made of Inconel 738LC Alloy, *Eng. Fail. Anal.*, Vol. 12, No. 3, pp. 474-486.
- McAlister, A.J. and Kahan, D. J. (1986). The Al-Pt (Aluminium-Platinum) System, *Bulletin of Alloy Phase Diagrams*, Vol. 7, pp. 45-51.
- Merker, J., Fischer, B., Völkl, R. and Lupton, D.F. (2003). Investigations of New Oxide Dispersion Hardened Platinum Materials in Laboratory Tests and Industrial Applications, *Materials Science Forum*, Vol. 426-432, pp. 1979-1984.

- Müller, J. and Neuschütz, D. (2003). Efficiency of α -alumina as diffusion barrier between bond coat and bulk material of gas turbine blades, *Vacuum*, Vol. 71, No. 1-2, pp. 247-251.
- Müller, L., Glatzel U. and Feller-Kniepmeier, M. (1993). Calculation of the Internal Stresses and Strains in the Microstructure of a Single-Crystal Nickel-Base Superalloy During Creep, *Acta Metallurgica et Materialia*, Vol. 41, No. 12, pp. 3401-3411.
- NIMS (2007). Research and Development of Superalloys for Aeroengine Applications, Date of access: 5 May 2010. Available from: National Institute of Materials Science website: http://sakimori.nims.go.jp/topics/hightemp_e.pdf
- Ochiai, S. (Ed.) (1994). Dispersion-Strengthened Materials- Platinum-Based Alloys, In: *Mechanical Properties of Metallic Composites*, Marcel Dekker Inc., New York, pp. 341-371. Cited by Cornish et al., 2009b.
- Oya, Y., Mishima, U. and Suzuki, T. (1987). $L1_2 \leftrightarrow D0_c$ Martensitic Transformation in Pt_3Al and Pt_3Ga , *Zeitschrift für Metallkunde*, Vol. 78, No. 7, pp. 485-490.
- Panfilov, P., Pilugin, V.P. and Antonova, O.V. (2008). On Specific Feature of Plastic Deformation in Ir, in: *Creep 2008: 11th Int. Conf. on Creep and Fracture of Engineering Materials and Structures, Book of Abstracts*, Bayreuth, Germany, 4-9 May, p. CP-131.
- Panayotou, N.F. (1982). The use of microhardness to determine the strengthening and microstructural alterations of 14 MeV neutron irradiated metals, *J. of Nuclear Materials*, Vol. 108, pp. 456-462.
- Pather, R., Mitten, W.A., Holdway, P., Ubhi, H.S. and Wisbey, W.A. (2003). Effect of High Temperature Environment on High Strength Titanium Aluminide Alloy, *Proc. Advanced Materials and Processes for Gas Turbines*, TMS, pp. 309-316, 22-26 Sep. 2002, Copper Mountain, Colorado, USA. ISBN 0-97339-556-5.
- Pint, B. A., DiStefano J. R. and Wright, I. G. (2006). Oxidation resistance: One barrier to moving beyond Ni-base superalloys, *Mat. Sci. and Eng. A*, Vol. 415, No. 1-2, pp. 255-263.
- Plansee (1998). Dispersion-Strengthened High-Temperature Materials, Plansee brochure, Lechbruck.
- Potgieter, J.H., van Bennekom, A. and Ellis, P. (1995). Investigation of the Active Dissolution Behaviour of a 22% Chromium Duplex Stainless Steel with Small Ruthenium Additions in Sulphuric Acid, *ISIJ Int.*, Vol. 35, pp. 197-202.
- Potgieter, J.H., Maledi, N.B., Sephton, M. and Cornish, L.A. (2010). The Platinum Development Initiative: Platinum-Based Alloys for High Temperature and Special Applications: Part IV - Corrosion, *Platinum Metals Review*, Vol. 54, No. 2, pp. 112-119.
- Purvis, A.L. and Warnes, B. M. (2001). The effects of platinum concentration on oxidation resistance of superalloys coated with single-phase platinum aluminide, *Surf. and Coat. Tech.*, Vol. 146, pp. 1-6.
- Qiu, Y.Y. (1996). The effect of the lattice strains on the directional coarsening of γ' precipitates in Ni-based alloys, *J. of Alloys and Compounds*, Vol. 232, No. 10, pp. 254-263.
- Roehrig, F.K. (1981). Owens-Corning Fiberglass Corp., *World Patent Appl.* 81/00,977.
- Rhys-Jones, T.N. (1989). Coatings for blade and vane applications in gas turbines, UK Corrosion '87-High Temperature Materials, *Corrosion Science*, vol. 29, no. 6, pp. 623-646.

- Rudnik, Y., Völkl, R., Vorberg, S. and Glatzel, U. (2008). The effects of Ta additions on the phase compositions and high temperature properties of Pt base alloys, *Mat.Sci. and Eng. A*, Vol. 479, pp. 306-312.
- Saltykov, P., Fabrichnaya, O., Golczewski, J. and Aldinger, F. (2004). Thermodynamic Modeling of Oxidation of Al-Cr-Ni Alloys, *J. of Alloys and Compounds*, Vol. 381, No. 1-2, pp. 99-113.
- Santamarta, R. R. Neethling, R., Schryvers D. and Douglas, A. (2003). HRTEM investigation of the low temperature phase of Pt₃Al precipitates in (Pt), In *Proc. Microsc. Soc. south. Afr.*, Vol. 32, Cape Town, 3-5 Dec. 2003, p. 15.
- Schubert, K. (1964). *Kristallstrukturen Zweikomponentiger Phasen*, Springer Verlag OHG, 1st edn., Berlin, Germany, p. 30.
- Selman, G.L. and Darling, A.S. (1973). Johnson Matthey PLC, *British Patent* 1,340,076.
- Shing T.L., Luyckx, S., Northrop, I.T. and Wolff, I. (2001). The Effect of Ruthenium additions on the hardness, toughness and grain size of WC-Co, *Int. J. of Refractory Metals and Hard Materials*, Vol. 19, pp. 41-44.
- Shongwe, M.B., Cornish, L.A. and Süß, R. (2009). Effect of Misfit on the Microstructure of Pt Based Superalloys, *Proc. Microsc. Soc. south. Afr.*, Vol. 39, p. 59, Durban, South Africa, 8-11 Dec. 2009, ISSN 0250-0418.
- Shongwe, M.B., Odera, B., Samal, S., Ukpong, A.M., Watson, A., Süß, R., Chown, L.H., Rading, G.O. and Cornish, L.A. (2010). Assessment of Microstructures in the Development of Pt-based Superalloys, *Light Metals Conference, SAIMM*, Paper 184-202 Shongwe on CD, Muldersdrift, Johannesburg, 27-29 Oct. 2010.
- Sidhu, B. S. and Prakash, S. (2006). Studies on the behaviour of stellite-6 as plasma sprayed and laser remelted coatings in molten salt environment at 900 °C under cyclic conditions, *Materials Process Technology*, Vol. 172, No. 1, pp. 52-63.
- Sidhu, T.S., Agrawal, R.D. and Prakash, S. (2005). Hot Corrosion of Some Superalloys and Role of High-Velocity Oxy-Fuel Spray Coatings - A Review, *Surf. Coat.s Tech.*, Vol. 198, pp. 441-446.
- Sidhu, T. S., Prakash S. and Agrawal, R.D. (2006). Hot Corrosion and Performance of Nickel Based Coatings, *Current Science*, Vol. 90, No. 1, pp. 41-47.
- Sims, C.T., Stoloff, N.S. and Hagel W.C. (1987). *Superalloys II: High Temperature Materials For Aerospace and Industrial Power*, Wiley-Interscience, New York, USA, 1987.
- Süß, R., Hill, P.J., Ellis, P. and Wolff I.M. (2001a). The Oxidation Resistance of Pt-Base γ/γ' Analogues to Ni-Base Superalloys, In: *Proc. 7th European Conf. on Advanced Materials and Processes*, Rimini, Italy, 10-14 June, 2001. Paper No. 287, CD-ROM, ISBN 8885298397.
- Süß, R., Hill, P.J., Ellis, P. and Cornish, L.A. (2001b). The oxidation resistance of Pt-Base superalloy Pt₈₀:Al₁₄:Cr₃:Ru₃ compared to that of Pt₈₆:Al₁₀:Cr₄, *Proc. Microsc. Soc. south. Afr.*, 2001, Johannesburg, Vol. 31, p. 21.
- Süß, R., Freund, D., Völkl, R., Fischer, B., Hill, P.J., Ellis, P., and Wolff, I.M. (2002). The creep properties of Pt-base γ/γ' analogues to Ni-base superalloys, *Mat. Sci. and Eng. A*, Vol. 338, pp. 133-141.
- Süß, R., Cornish, L.A., Hill, P.J., Hohls, J. and Compton, D.N (2003). Properties of a New Series of Superalloys Based on Pt₈₀:Al₁₄:Cr₃:Ru₃', in *Advanced Materials and Processes for Gas Turbines*, Ed. G. Fuchs, A. James, T. Gabb, M. McLean and H. Harada, TMS, 22-26 Sep. 2002, Copper Mountain, Colorado, USA, pp. 301-307.

- Süss, R. and Cornish, L.A. (2004). Tensile Test Properties of Pt-based Superalloys, *Beyond Ni-based Superalloys*, TMS 2004 133rd Annual Meeting and Exhibition, p. 269, Charlotte, North Carolina, USA, 14-16 Mar. 2004.
- Takeuchi, S. and Kuramoto, E. (1973). *Acta Met.*, Vol. 21, pg. 415, cited in Kamm, J.L. and Milligan, W.W. (1994).
- Tsaur, C.-C., Rock, J. C., Wang C.-J. and Su, Y.-H. (2005). The hot corrosion of 310 stainless steel with pre-coated NaCl/Na₂SO₄ mixtures at 750 °C, *Mat. Chem. and Phys.*, Vol. 89, No. 2-3, pp. 445-453.
- van der Lingen, E. and Sandenbergh, R.F. (2001). The cathodic modification behaviour of Ru additions to titanium in hydrochloric acid, *J. of Corrosion Science*, Vol. 43, pp. 577-590.
- Vattré, A., Devincere, B. and Roos, A. (2009). Dislocation dynamics simulations of precipitation hardening in Ni-based superalloys with high γ' volume fraction, *Intermetallics*, Vol. 7, No. 12, pp. 988-994.
- Völkl, R. Glatzel U. and Feller-Kniepmeier, M. M. (1998). Measurement of the Lattice Misfit in the Single Crystal Nickebase Superalloys CMSX-4, SRR 99 and SC 16 by Convergent Beam Electron Diffraction, *Acta Materialia*, Vol. 46, No. 12, pp. 4395-4404.
- Völkl, R., Freund, D., Fischer, B. and Gohlke, D. (1999). Comparison of the creep and fracture behaviour of non-hardened and oxide dispersion hardened platinum base alloys at temperatures between 1200°C and 1700°C, *Proc. 8th Int. Conf. on Creep and Fracture of Engineering Materials and Structures*, Vol. 171-174, pp. 77-84.
- Völkl, R., Freund, D., Behrends, A., Fischer, B., Merker, J. and Lupton, D. (2000). Platinum Base Alloys for High Temperature Space Applications, In: *Euromat 99 Series: Materials for Transport*, ed. P.J. Winkler, Wiley-VCH Verlag GmbH, Weinheim.
- Völkl, R. and Fischer, B. (2004). Mechanical Testing of Ultra-High Temperature Alloys, *Experimental Mechanics*, Vol. 44, No. 2, pp. 121-127.
- Völkl, R. Yamabe-Mitarai, Y. Huang C. and Harada, H. (2005). Stabilizing the L1₂ structure of Pt₃Al(r) in the Pt-Al-Sc system, *Met. Mat. Trans. A*, Vol. 36, No. 11, pp. 2881-2892.
- Völkl, R., Wenderoth, M., Preussner, J., Vorberg, S., Fischer, B., Yamabe-Mitarai, Y., Harada, H. and Glatzel, U. (2009). Development of a precipitation-strengthened Pt-base alloy, *Mat. Sci. and Eng. A*, Vol. 510-511, pp. 328-331.
- Vorberg, S., Wenderoth, M., Fischer, B., Glatzel U. and Völkl, R. (2004). Pt-Al-Cr-Ni superalloys: heat treatment and microstructure, *JOM*, Vol. 56, No. 9, pp. 40-43.
- Vorberg, S., Wenderoth, M., Fischer, B., Glatzel U. and Völkl, R. (2005). A TEM investigation of the γ/γ' phase boundary in Pt-based superalloys, *JOM*, Vol. 57, No. 3, pp. 49-51.
- Wenderoth, M., Cornish, L.A., Süss, R., Vorberg, S., Fischer, B., Glatzel, U. and Völkl, R. (2005). On the Development and Investigation of Quaternary Pt-Based Superalloys with Ni Additions, *Met. Mat. Trans. A*, Vol. 36, pp. 567-575.
- Wenderoth, M., Völkl, R., Yokokawa, T., Yamabe-Mitarai Y. and Harada, H. (2006). High temperature strength of Pt-base superalloys with different γ' volume fractions, *Scripta Materialia*, Vol. 54, No. 2, pp. 275-279.
- Wenderoth, M., Völkl, R., Vorberg, S., Yamabe-Mitarai, Y., Harada, H. and Glatzel, U. (2007). Micro-structure, oxidation resistance and high temperature strength of γ' hardened Pt base alloys, *Intermetallics*, Vol. 15, pp. 539-549.

- Westbrook, J.H. (1958). Precipitation of Ni₃Al from nickel solid solution as octahedrally doped cubes, *Zeitschrift für Kristallographie*, Vol. 110, pp. 21-29.
- Whalen, M.V. (1988). Space Station Resistojets, *Plat. Met.Rev.*, Vol. 32, No. 1, pp. 2-10.
- Wolff, I.M. and Hill, P.J. (2000). Platinum metals-based intermetallics for high-temperature service, *Platinum Metals Review*, Vol. 44, No. 4, pp. 158-166.
- Wood, G. and Stott, F. (1987). Oxidation of alloys, *Mat. Sci. and Tech.*, Vol. 3, No. 7, pp. 519-530.
- Yamabe, Y., Koizumi, Y., Murakami, H., Ro, Y., Maruko, T. and Harada, H. (1996). Development of Ir-base Refractory Superalloys, *Scripta Met.*, Vol. 35, No. 2, pp. 211-215.
- Yamabe-Mitarai, Y., Koizumi, Y., Murakami, H., Ro, Y., Maruko, T. and Harada, H. (1997). Rh-base Refractory Superalloys for Ultra-high Temperature Use, *Scripta Met.*, Vol. 36, No. 4, pp. 393-398.
- Yamabe-Mitarai, Y., Ro, Y., Harada, H. and Maruko, T. (1998). Ir-base Refractory Superalloys for Ultra-High Temperature Use, *Met. Trans. A*, Vol. 29, No. 2, pp. 537-549.
- Yamabe-Mitarai, Y., Ro, Y., Maruko, T. and Harada, H. (1999). Microstructure dependence of strength of Ir-base refractory superalloys, *Intermetallics*, Vol. 7, No. 1, pp. 49-58.
- Yamabe-Mitarai, Y., Ro, Y., Maruko, T. and Harada, H. (1998). Precipitation hardening of Ir-Nb and Ir-Zr alloys, *Scripta Materiala*, Vol. 40, No. 1, pp. 109-115.
- Yamabe-Mitarai, Y. and Aoki, H. (2003). An assessment of Pt-Ir-Al alloys for high-temperature materials, *J.of Alloys and Compounds*, Vol. 359, pp. 143-152.
- Yoshida, M. (1993). Effect of hot corrosion on the mechanical performances of superalloys and coatings systems, *Corrosion Science*, Vol. 35, No. 5-8, pp. 1115-1124.
- Yu, X.H., Yamabe-Mitarai, Y., Ro, Y. and Harada, H. (2000). Design of quaternary Ir-Nb-Ni-Al refractory superalloys, *Met. and Mat.Trans. A*, Vol. 31A, No. 1, pp. 173-178A.
- Zhang, X-F. and Zhang, Z. (Eds.) (2001). *Progress In Transmission Electron Microscopy: Concepts and Techniques*, Vol. 1, Springer-Verlag, Germany, pg. 263.
- Zhao, J-C., Jackson, M., Peluso, L. and Brewer, L. N. (2002). A Diffusion Multiple Approach for the Accelerated Design of Structural Materials, *MRS Bulletin*, Vol. 27, pp. 324-329.
- Zhao, J-C. and Westbrook, J.H. (2003). Ultra high temperature materials for jet engines, *MRS Bulletin*, Vol. 28, No. 9, pp. 622-627.
- Zheng, D., Zhu, S. and Wang, F. (2006). Oxidation and hot corrosion behavior of a novel enamel-Al₂O₃ composite coating on K38G superalloy, *Surf. Coat. Tech.*, Vol. 200, No. 20-21, pp. 5931-5936.



Advances in Gas Turbine Technology

Edited by Dr. Ernesto Benini

ISBN 978-953-307-611-9

Hard cover, 526 pages

Publisher InTech

Published online 04, November, 2011

Published in print edition November, 2011

Gas turbine engines will still represent a key technology in the next 20-year energy scenarios, either in stand-alone applications or in combination with other power generation equipment. This book intends in fact to provide an updated picture as well as a perspective vision of some of the major improvements that characterize the gas turbine technology in different applications, from marine and aircraft propulsion to industrial and stationary power generation. Therefore, the target audience for it involves design, analyst, materials and maintenance engineers. Also manufacturers, researchers and scientists will benefit from the timely and accurate information provided in this volume. The book is organized into five main sections including 21 chapters overall: (I) Aero and Marine Gas Turbines, (II) Gas Turbine Systems, (III) Heat Transfer, (IV) Combustion and (V) Materials and Fabrication.

How to reference

In order to correctly reference this scholarly work, feel free to copy and paste the following:

Lesley A. Cornish and Lesley H. Chown (2011). Platinum-Based Alloys and Coatings: Materials for the Future?, *Advances in Gas Turbine Technology*, Dr. Ernesto Benini (Ed.), ISBN: 978-953-307-611-9, InTech, Available from: <http://www.intechopen.com/books/advances-in-gas-turbine-technology/platinum-based-alloys-and-coatings-materials-for-the-future->

INTECH
open science | open minds

InTech Europe

University Campus STeP Ri
Slavka Krautzeka 83/A
51000 Rijeka, Croatia
Phone: +385 (51) 770 447
Fax: +385 (51) 686 166
www.intechopen.com

InTech China

Unit 405, Office Block, Hotel Equatorial Shanghai
No.65, Yan An Road (West), Shanghai, 200040, China
中国上海市延安西路65号上海国际贵都大饭店办公楼405单元
Phone: +86-21-62489820
Fax: +86-21-62489821

© 2011 The Author(s). Licensee IntechOpen. This is an open access article distributed under the terms of the [Creative Commons Attribution 3.0 License](#), which permits unrestricted use, distribution, and reproduction in any medium, provided the original work is properly cited.

IntechOpen

IntechOpen